

FULLY DISCRETE FINITE ELEMENT APPROXIMATIONS OF THE NAVIER–STOKES–CAHN–HILLIARD DIFFUSE INTERFACE MODEL FOR TWO-PHASE FLUID FLOWS*

XIAOBING FENG†

Abstract. This paper develops and analyzes some fully discrete finite element methods for a parabolic system consisting of the Navier–Stokes equations and the Cahn–Hilliard equation, which arises as a diffuse interface model for the flow of two immiscible and incompressible fluids. In the model the two sets of equations are coupled through an extra phase induced stress term in the Navier–Stokes equations and a fluid induced transport term in the Cahn–Hilliard equation. Fully discrete mixed finite element methods are proposed for approximating the coupled system, it is shown that the proposed numerical methods satisfy a mass conservation law, and a discrete energy law which is analogous to the basic energy law for the phase field model. The convergence of the numerical solutions to the solutions of the phase field model and its sharp interface limit is established by utilizing the discrete energy law. As a by-product, the convergence result also provides a constructive proof of the existence of weak solutions to the Navier–Stokes–Cahn–Hilliard phase field model. Numerical experiments are also presented to validate the theory and to show the effectiveness of the combined phase field and finite element approach.

Key words. two-phase fluids, phase field model, Cahn–Hilliard equation, Navier–Stokes equations, finite element methods

AMS subject classifications. 65M60, 35K55, 76D05

DOI. 10.1137/050638333

1. Introduction. Interfacial dynamics in the mixture of different fluids, solids, or gas has been one of the fundamental issues in hydrodynamics and materials science. It plays an increasingly important role in many current scientific, engineering, and industrial applications (cf. [7, 15] and the references therein). In the classical approaches, the interface is usually considered as a free curve/surface that evolves in time along with fluid. The movement of the interface at each time is determined by a set of interfacial balance conditions. In the case of two immiscible incompressible fluids, the dynamics of the fluid mixture is described by the following two-phase Navier–Stokes equations:

$$(1.1) \quad \mathbf{u}_t - \nu \Delta \mathbf{u} + (\mathbf{u} \cdot \nabla) \mathbf{u} + \nabla p = \mathbf{g} \quad \text{in } \Omega_T \setminus \Gamma_t,$$

$$(1.2) \quad \operatorname{div} \mathbf{u} = 0 \quad \text{in } \Omega_T \setminus \Gamma_t,$$

$$(1.3) \quad [(\nu D(\mathbf{u}) - pI)\mathbf{n}] = \alpha \kappa \mathbf{n} \quad \text{on } \Gamma_t,$$

$$(1.4) \quad [\mathbf{u}] = 0 \quad \text{on } \Gamma_t,$$

with a given set of initial and boundary conditions. Here $\Omega \subset \mathbf{R}^d$ ($d = 1, 2, 3$) is a bounded domain, $\Omega_T = \Omega \times (0, T)$, Γ_t denotes the (free) interface at the time t with the normal \mathbf{n} and the mean curvature κ , $\alpha > 0$ is the surface tension constant. $D(\mathbf{u}) = \frac{1}{2}(\nabla \mathbf{u} + (\nabla \mathbf{u})^T)$ denotes the deformation tensor, I is the $d \times d$ identity matrix. $[\mathbf{u}]$ denotes the jump of the \mathbf{u} across the interface Γ_t . Clearly, (1.3) and (1.4) are the

*Received by the editors August 17, 2005; accepted for publication (in revised form) December 5, 2005; published electronically June 2, 2006. This work is partially supported by the NSF grant DMS-0410266.

<http://www.siam.org/journals/sinum/44-3/63833.html>

†Department of Mathematics, The University of Tennessee, Knoxville, TN 37996 (xfeng@math.utk.edu).

interfacial conditions for the fluid mixture, which are the mathematical descriptions of the balance of the normal stress and the balance of the movement.

Computationally, the above free interface problem is difficult to solve directly due to the existence of the surface tension on the interface. In addition, during the evolution the fluid interface may experience topological changes such as self-intersection, pinch-off, splitting, and fattening. When that happens, the classical solution of the free interface problem ceases to exist. In such a situation it is delicate and difficult to develop a proper notion of generalized solutions, it becomes even more challenging to compute the generalized solutions when they are defined.

To overcome the difficulties, an alternative approach for solving interface problems is the *diffuse interface (or mean field) theory*, which was originally developed as methodology for modeling and approximating solid-liquid phase transitions in which the effects of surface tension and nonequilibrium thermodynamic behavior may be important at the surface [28, 12, 24]. In the theory, the interface is represented as a thin layer of finite thickness. The method uses an auxiliary function (called phase field function/variable) to indicate the “phase.” The phase-field function assumes distinct values in the bulk phases away from the interfacial regions over which the phase function varies smoothly, and the interface itself can be associated with an intermediate contour or level set of the phase function (cf. [32] and the references therein). The diffuse interface models converge to their corresponding sharp interface models as the width of the interfacial layer ε tends to zero.

This is the second paper in a series (cf. [18]) which devotes to finite element numerical analysis of two-phase fluid flows based on the phase field (diffuse interface) approach. In [18] finite element methods were developed and analyzed for the Navier–Stokes–Allen–Cahn phase field model proposed in. The goal of this paper is to carry out a parallel finite element numerical analysis for a mass-conserved diffuse interface model for two-phase fluids proposed in [27, 30], which consists of the Navier–Stokes equations and the Cahn–Hilliard equation. In the model the two sets of equations are coupled through an extra phase induced stress term in the Navier–Stokes equations and a fluid induced transport term in the Cahn–Hilliard equation. We develop and analyze some fully discrete mixed finite element methods for the Navier–Stokes–Cahn–Hilliard phase field model. It is proved that the proposed numerical methods satisfy a mass conservation law, and a discrete energy law which exactly mimics the basic energy law for the phase field model. The convergence of the numerical solutions to the solutions of the phase field model and its sharp interface limit is then established by utilizing the discrete energy law.

It should be noted that the Navier–Stokes–Cahn–Hilliard phase field model (in different forms, see section 2 for more details) for two phase fluids has been studied numerically by several authors [2, 3, 27, 30, 31], among them [27, 30] are most closely related to the current paper. In [27] Jacqmin derived the mathematical model based on physical arguments, and then proposed some finite difference compact schemes for the model. Impressive numerical experiments also were reported in the paper although no convergence analysis was given. In [30], inspired by their early experiences on the nematic liquid crystal flows, Liu and Shen rederived the Navier–Stokes–Cahn–Hilliard phase field model based on the (heuristic) mathematical arguments, and then proposed some Fourier-spectral element methods under the periodic assumptions. *Local-in-time* stability estimates were also established for the proposed Fourier-spectral element methods.

The remainder of this paper is organized as follows. In section 2, we present the mass conserved Navier–Stokes–Cahn–Hilliard phase field model for two-phase fluids

to be studied in this paper. We then demonstrate that various phase field models appeared in [27, 30] are actually mathematically equivalent up to an additive function to the pressure. However, it is shown later in this paper that numerically the phase field model in the potential form is favored since finite element methods based on this form are shown to fulfill a *global-in-time* energy (or stability) estimate which exactly mimics the basic energy law of the differential model. In section 3, we first re-establish the basic energy law (in a slightly different form) associated with the Navier–Stokes–Cahn–Hilliard phase field model, and then derive some additional a priori energy estimates which show explicit dependence on the physical parameters $\varepsilon, \lambda, \gamma$, and ν . In section 4, we propose and analyze a family of fully discrete mixed finite element methods for the phase field model. It is proved that the proposed numerical methods enjoy a discrete energy law which mimics the basic energy law for the differential problem. It is this discrete energy law which paves the way for us to establish the convergence of the fully discrete methods to the phase field model as the mesh sizes $h, \tau \rightarrow 0$, and to the sharp interface model (1.1)–(1.4) as the mesh sizes h, τ , and the capillary width ε all tend to zero, provided that the phase field model converges to the sharp interface model. Our main idea is to rewrite the flow equations in the potential form by introducing a new “pressure” $\bar{p} = p + \frac{\lambda}{2}|\nabla\varphi|^2 + \frac{\lambda}{\varepsilon^2}F(\varphi) + \lambda\varphi(\Delta\varphi - \frac{1}{\varepsilon^2}F'(\varphi))$ in the place of the original pressure p . As a by-product, our convergence result also provides a rigorous proof of the existence of weak solutions to the phase field model, which clearly is of interests in itself. Finally, in section 5 we present some numerical experiment results to validate our theoretical results and to show the effectiveness of the combined phase field and finite element approach.

2. The Navier–Stokes–Cahn–Hilliard phase field model. The phase field model for two immiscible and incompressible fluids with comparable densities (which are taken to be 1) and viscosities $\nu > 0$ to be studied in this paper takes the form [30, 3]

$$(2.1) \quad \mathbf{u}_t - \nu\Delta\mathbf{u} + (\mathbf{u} \cdot \nabla)\mathbf{u} + \nabla p + \lambda \operatorname{div}(\nabla\varphi \otimes \nabla\varphi) = \mathbf{g} \quad \text{in } \Omega_T,$$

$$(2.2) \quad \varphi_t + \mathbf{u} \cdot \nabla\varphi + \gamma\Delta(\Delta\varphi - \frac{1}{\varepsilon^2}f(\varphi)) = 0 \quad \text{in } \Omega_T,$$

$$(2.3) \quad \operatorname{div} \mathbf{u} = 0 \quad \text{in } \Omega_T.$$

To close the system, it will be complemented with the following initial and boundary conditions:

$$(2.4) \quad \mathbf{u}(\cdot, 0) = \mathbf{u}_0^\varepsilon(\cdot), \quad \varphi(\cdot, 0) = \varphi_0^\varepsilon(\cdot), \quad \text{in } \Omega,$$

$$(2.5) \quad \mathbf{u} = 0, \quad \frac{\partial\varphi}{\partial\mathbf{n}} = \frac{\partial\Delta\varphi}{\partial\mathbf{n}} = 0, \quad \text{on } \partial\Omega_T := \partial\Omega \times (0, T].$$

Note that we have suppressed the superscript ε in $(\mathbf{u}^\varepsilon, \varphi^\varepsilon, p^\varepsilon)$ for the notation brevity. Here the vector $\mathbf{u}(x, t) \in \mathbf{R}^d$ and the scalar $p(x, t) \in \mathbf{R}$ denote the velocity and the pressure of the fluid mixture at the space time point (x, t) , respectively. The scalar function φ is called a *phase function* and is used to indicate the fluid phases. φ assumes distinct values in the bulk phases away from a thin layer (called the interfacial region) over which φ varies smoothly, and the interface itself can be associated with the zero level set $\{\varphi = 0\}$ of φ ($f(\varphi) = F'(\varphi)$ and $F(\varphi) = \frac{1}{4}(\varphi^2 - 1)^2$). The positive constants λ, γ , and ε are the surface tension, the elastic relaxation time, and the capillary width (width of the interfacial layer), respectively. $\nabla\varphi \otimes \nabla\varphi$ stands for the $d \times d$ rank-one matrix $(\nabla\varphi)^T \nabla\varphi$ with entries $\varphi_{x_i} \varphi_{x_j}$. We especially note that $\varepsilon \ll 1$.

Equation (2.1) without the stress term $\lambda \operatorname{div} (\nabla \varphi \otimes \nabla \varphi)$ is the Navier–Stokes equations [33] and (2.2) without the convection term $\mathbf{u} \cdot \nabla \varphi$ is the Cahn–Hilliard equation [23, 32]. In the literature, the phase equation is always given by (2.2). On the other hand, the flow equations often appear differently in different papers due to how the phase induced force is expressed in the equations. In (2.1), since $\nabla \varphi \otimes \nabla \varphi$ is a phase induced stress tensor (its divergence represents the phase induced force), hence, we may regard (2.1) as the flow equations in the *stress form*. Using the differential identity

$$(2.6) \quad \operatorname{div} (\nabla \varphi \otimes \nabla \varphi) = \Delta \varphi \nabla \varphi + \frac{1}{2} \nabla |\nabla \varphi|^2,$$

(2.1) can be rewritten as

$$(2.7) \quad \mathbf{u}_t - \nu \Delta \mathbf{u} + (\mathbf{u} \cdot \nabla) \mathbf{u} + \nabla \hat{p} + \lambda \Delta \varphi \nabla \varphi = \mathbf{g},$$

where

$$(2.8) \quad \hat{p} := p + \frac{\lambda}{2} |\nabla \varphi|^2.$$

By introducing the *chemical potential* (cf. [11, 23, 32]),

$$(2.9) \quad w := -\Delta \varphi + \frac{1}{\varepsilon^2} f(\varphi),$$

and noticing the fact that $F'(\varphi) = f(\varphi)$, (2.7) can be rewritten as

$$(2.10) \quad \mathbf{u}_t - \nu \Delta \mathbf{u} + (\mathbf{u} \cdot \nabla) \mathbf{u} + \nabla \tilde{p} - \lambda w \nabla \varphi = \mathbf{g},$$

where

$$(2.11) \quad \tilde{p} := \hat{p} + \frac{\lambda}{\varepsilon^2} F(\varphi) = p + \frac{\lambda}{2} |\nabla \varphi|^2 + \frac{\lambda}{\varepsilon^2} F(\varphi).$$

It was based exactly on $(\mathbf{u}, \tilde{p}, \varphi, w)$ formulation that convergent finite element methods were successfully developed in [18] for the related Navier–Stokes–Allen–Cahn phase field model of for two-phase fluids.

It is natural to ask if the success of [18] can be extended to the above Navier–Stokes–Cahn–Hilliard phase field model. It turns out (see section 4 for details) that one can show that mixed finite methods based on $(\mathbf{u}, \tilde{p}, \varphi, w)$ formulation for the Navier–Stokes–Cahn–Hilliard phase field model do satisfy a discrete energy law which mimics the basic energy law associated with the phase field model. However, the numerical solutions may *not* satisfy the mass conservation law

$$\int_{\Omega} \varphi(x, t) dx = \int_{\Omega} \varphi(x, 0) dx \quad \forall t \in [0, T],$$

associated with the Navier–Stokes–Cahn–Hilliard phase field model (2.1)–(2.5).

To overcome the difficulty, we define another new “pressure” \bar{p} as

$$(2.12) \quad \bar{p} := \tilde{p} - \lambda \varphi w = p + \frac{\lambda}{2} |\nabla \varphi|^2 + \frac{\lambda}{\varepsilon^2} F(\varphi) + \lambda \varphi \left(\Delta \varphi - \frac{1}{\varepsilon^2} F'(\varphi) \right),$$

and rewrite (2.10) as

$$(2.13) \quad \mathbf{u}_t - \nu \Delta \mathbf{u} + (\mathbf{u} \cdot \nabla) \mathbf{u} + \nabla \bar{p} + \lambda \varphi \nabla w = \mathbf{g},$$

which it turns out is exactly the flow equations proposed by Jacqmin in [27] using physical arguments. Since the phase induced force is expressed as the gradient of the chemical potential w , we may regard (2.13) as the flow equation in the *potential form*. We also note that with help of the chemical potential w , (2.2) can be rewritten as

$$(2.14) \quad \varphi_t + \mathbf{u} \cdot \nabla \varphi - \gamma \Delta w = 0.$$

Equations (2.9) and (2.14) is known as the mixed (or split) formulation for the Cahn–Hilliard equation (cf. [16, 19, 20]).

In section 4, we shall present some fully discrete mixed finite element methods for the Navier–Stokes–Cahn–Hilliard phase field model based on the $(\mathbf{u}, \bar{p}, \varphi, w)$ formulation, which consists of (2.13), (2.14), (2.3), and (2.9). It is shown that such numerical methods not only satisfy the global-in-time discrete energy law but also fulfill the mass conservation law. We like to emphasize that although the flow equations presented above all are mathematically equivalent, numerical methods based on these equations are often different, and the differences could be significant.

3. A priori energy estimates. The standard space notations are used in this paper; we refer to [1, 33] for their exact definitions. In particular, B^* denotes the dual space of a Banach space B , and \mathbf{B} denotes the vector Banach space B^d . (\cdot, \cdot) is used to denote the standard $L^2(\Omega)$ inner product, $\langle \cdot, \cdot \rangle$ stands for the dual product between $H_0^1(\Omega)$ and $H^{-1}(\Omega)$, and

$$L_0^2(\Omega) = \{q \in L^2(\Omega); (q, 1) = 0\},$$

$$\mathbf{V} = \{\mathbf{v} \in \mathbf{H}_0^1(\Omega); \operatorname{div} \mathbf{v} = 0 \text{ in } \Omega\},$$

$$\mathbf{H} = \{\mathbf{v} \in \mathbf{L}^2(\Omega); \operatorname{div} \mathbf{v} = 0 \text{ in } \Omega \text{ and } \mathbf{v} \cdot \mathbf{n}|_{\partial\Omega} = 0\}.$$

In addition, we use π to denote the L^2 -orthogonal projection from $\mathbf{L}^2(\Omega)$ onto \mathbf{H} , and $\tilde{\Delta} = \pi\Delta$ to denote the Stokes operator (cf. [33]).

Throughout the paper, unless stated otherwise, c and C will be used to denote generic positive constants which is independent of \mathbf{u}, p, φ , and ε .

Existence and uniqueness (for $d = 2$) of weak solutions of system (2.1)–(2.3) were heuristically outlined in [30]. A key ingredient of the proof is to establish the basic energy law for the phase field model (see (3.9) below). In this section, we shall first reestablish the basic energy law in a slightly different form. We shall also derive some additional uniform (in ε) a priori estimates, in particular on \mathbf{u}_t, φ_t , and \bar{p} , for weak solutions to the system (2.1)–(2.3), which will be needed in section 4. Special attention will be given to tracing the explicit dependence of the a priori estimates on the capillary width ε , and the parameters λ and γ .

LEMMA 3.1. *Suppose that $\mathbf{g} \in L^2((0, T); \mathbf{L}^2(\Omega))$, and the initial values \mathbf{u}_0^ε and φ_0^ε satisfy $|\varphi_0^\varepsilon| \leq 1$ and $\mathcal{J}_{\varepsilon, \lambda}(\mathbf{u}_0^\varepsilon, \varphi_0^\varepsilon) < \infty$, i.e., the initial energy is bounded, then every regular solution (\mathbf{u}, φ, p) of system (2.1)–(2.3) satisfies the following estimates: for all $T \in [0, \infty]$*

$$(3.1) \quad \int_{\Omega} \varphi(x, t) dx = \int_{\Omega} \varphi_0^\varepsilon(x) dx \quad \forall t \in (0, T),$$

$$(3.2) \quad \operatorname{ess\,sup}_{t \in [0, T]} \{\|\mathbf{u}(t)\|_{L^2}^2 + \lambda \|\nabla \varphi(t)\|_{L^2}^2 + \lambda \varepsilon^{-2} (F(\varphi(t)), 1)\} \leq C,$$

$$(3.3) \quad \int_0^T \nu \|\nabla \mathbf{u}(t)\|_{L^2}^2 dt + \left\{ \int_0^T \lambda \gamma \|\nabla w(t)\|_{L^2}^2 dt + \int_0^T \lambda \gamma^{-1} \|\varphi_t(t) + \mathbf{u}(t) \cdot \nabla \varphi(t)\|_{H^{-1}}^2 dt \right\} \leq C,$$

$$(3.4) \quad \int_0^T \left\{ \|\mathbf{u}_t(t)\|_{V^*}^{\frac{12}{6+d}} + \|\mathbf{u}_t(t)\|_{(V \cap L^\infty)^*}^2 \right\} dt \leq C,$$

$$(3.5) \quad \operatorname{ess\,sup}_{t \in [0, T]} \left\| \int_0^t \bar{p}(s) ds \right\|_{L^2} \leq C,$$

$$(3.6) \quad \int_0^T \|\varphi_t(t)\|_{H^{-1}}^2 dt \leq C,$$

where $\bar{p} = p + \frac{\lambda}{2} |\nabla \varphi|^2 + \frac{\lambda}{\varepsilon^2} F(\varphi)$. In addition, there holds

$$(3.7) \quad \int_0^T \|\Delta \varphi(t)\|_{L^2}^2 dt \leq C \varepsilon^{-2},$$

$$(3.8) \quad \int_0^T \|\nabla \Delta \varphi\|_{L^2}^2 dt \leq C \varepsilon^{-\frac{6(4+d)}{6-d}}.$$

Proof. Testing (2.1) with \mathbf{u} , (2.14) with $\lambda \gamma^{-1} \Delta^{-1}(\varphi_t + \mathbf{u} \cdot \nabla \varphi)$ or with w , (2.9) with φ_t , using the differential identity (2.6), and adding the resulting equations yield

$$(3.9) \quad \frac{d}{dt} \mathcal{J}_{\varepsilon, \lambda}(\mathbf{u}, \varphi) + \nu \|\nabla \mathbf{u}\|_{L^2}^2 + \left\{ \lambda \gamma \|\nabla w\|_{L^2}^2 + \nu \gamma^{-1} \|\varphi_t + \mathbf{u} \cdot \nabla \varphi\|_{H^{-1}}^2 \right\} = \int_{\Omega} \mathbf{g} \cdot \mathbf{u} dx,$$

where

$$(3.10) \quad \mathcal{J}_{\varepsilon, \lambda}(\mathbf{u}, \varphi) := \int_{\Omega} \left[\frac{1}{2} |\mathbf{u}|^2 + \frac{\lambda}{2} |\nabla \varphi|^2 + \frac{\lambda}{\varepsilon^2} F(\varphi) \right] dx.$$

The identity (3.9) is known (cf. [27, 30]) as the basic energy law for the system (2.1)–(2.5).

Next, the estimates (3.2) and (3.3) follow easily from integrating (3.9) in t from 0 to T and using the inequality

$$|(\mathbf{g}, \mathbf{u})| \leq \frac{1}{4} \|\mathbf{u}\|_{L^2}^2 + \|\mathbf{g}\|_{L^2}^2.$$

To show (3.4), we test (2.13) with $\mathbf{v} \in \mathbf{V} \cap \mathbf{L}^\infty(\Omega)$ to get

$$(3.11) \quad \begin{aligned} (\mathbf{u}_t, \mathbf{v}) &= -\nu (\nabla \mathbf{u}, \nabla \mathbf{v}) - ((\mathbf{u} \cdot \nabla) \mathbf{u}, \mathbf{v}) - \lambda (\varphi \nabla w, \mathbf{v}) + (\mathbf{g}, \mathbf{v}) \\ &\leq \nu \|\nabla \mathbf{u}\|_{L^2} \|\nabla \mathbf{v}\|_{L^2} + \lambda \|\nabla w\|_{L^2} \|\varphi\|_{L^3} \|\mathbf{v}\|_{L^6} + \|\mathbf{g}\|_{L^2} \|\mathbf{v}\|_{L^2} \\ &\quad - ((\mathbf{u} \cdot \nabla) \mathbf{u}, \mathbf{v}). \end{aligned}$$

For the last term above we have

$$(3.12) \quad ((\mathbf{u} \cdot \nabla) \mathbf{u}, \mathbf{v}) \leq C \begin{cases} \|\nabla \mathbf{u}\|_{L^2}^{\frac{6+d}{6}} \|u\|_{L^2}^{\frac{6-d}{6}} \|\mathbf{v}\|_{L^6} + \|\nabla \mathbf{u}\|_{L^2} \|u\|_{L^2} \|\mathbf{v}\|_{L^6}, \\ \|\nabla \mathbf{u}\|_{L^2} \|u\|_{L^2} \|\mathbf{v}\|_{L^\infty}, \end{cases}$$

here we have used the interpolation inequality (cf. [1])

$$(3.13) \quad \|\mathbf{u}\|_{L^3} \leq C \|\nabla \mathbf{u}\|_{L^2}^{\frac{d}{6}} \|\mathbf{u}\|_{L^2}^{\frac{6-d}{d}} + C \|\mathbf{u}\|_{L^2}.$$

Equation (3.4) then follows from combining (3.11), (3.12), (3.13), (3.2), and (3.3).

To verify (3.5), testing (2.13) with $\mathbf{v} \in \mathbf{H}_0^1(\Omega)$ and integrating the resulted equation in t from 0 to $\tau (\leq T)$ yield

$$\begin{aligned} \left(\int_0^\tau p(t) dt, \operatorname{div} \mathbf{v} \right) &= (\mathbf{u}(\tau) - \mathbf{u}_0, \mathbf{v}) + \nu \left(\int_0^\tau \nabla \mathbf{u}(t) dt, \nabla \mathbf{v} \right) \\ &\quad + \left(\int_0^\tau (\mathbf{u} \cdot \nabla \mathbf{u})(t) dt, \mathbf{v} \right) - \lambda \left(\int_0^\tau (\varphi \nabla w)(t) dt, \mathbf{v} \right). \end{aligned}$$

Using the estimates (3.2), (3.3), (3.11)–(3.13), and the Sobolev inequality (cf. [1]) we conclude that

$$(3.14) \quad \left(\int_0^\tau p(t) dt, \operatorname{div} \mathbf{v} \right) \leq C \|\mathbf{v}\|_{H^1} \quad \forall \mathbf{v} \in \mathbf{H}_0^1(\Omega).$$

Equation (3.5) then follows from (3.14) and an application of the inf-sup inequality (cf. [33]).

To show (3.6), we first notice that $\nabla w \in L^2(\Omega_T)$ implies that $\Delta w \in L^2((0, T); H^{-1})$. Then (3.6) follows from (2.14), (3.2), (3.3), and the following inequality:

$$\|\mathbf{u} \cdot \nabla \varphi\|_{L^{\frac{6}{5}}} \leq \|\mathbf{u}\|_{L^3} \|\nabla \varphi\|_{L^2}.$$

To show (3.7), testing (2.9) with $\Delta \varphi$ we get

$$\begin{aligned} \|\Delta \varphi\|_{L^2}^2 &= -(w, \Delta \varphi) + \frac{1}{\varepsilon^2} (f(\varphi), \Delta \varphi) \leq \|\nabla w\|_{L^2} \|\nabla \varphi\|_{L^2} - \frac{1}{\varepsilon^2} (f'(\varphi), |\nabla \varphi|^2) \\ &\leq \left(\frac{1}{2} + \frac{1}{\varepsilon^2} \right) \|\nabla \varphi\|_{L^2}^2 + \frac{1}{2} \|\nabla w\|_{L^2}^2. \end{aligned}$$

Here we have used the fact that $f'(\varphi) = 3\phi^2 - 1$. The assertion then follows from the above inequality, (3.2), and (3.3).

Finally, applying the operator ∇ on both sides of (2.9) yields

$$\nabla \Delta \varphi = -\nabla w + \frac{1}{\varepsilon^2} f'(\varphi) \nabla \varphi = -\nabla w + \frac{3}{\varepsilon^2} \varphi^2 \nabla \varphi - \frac{1}{\varepsilon^2} \nabla \varphi,$$

which, (3.2), (3.3), and the interpolation inequality (cf. [1])

$$\|\varphi\|_{L^\infty} \leq C \left(\|\Delta \varphi\|_{L^2}^{\frac{d}{2(6-d)}} \|\varphi\|_{L^6}^{\frac{3(4-d)}{2(6-d)}} + \|\varphi\|_{L^6} \right)$$

imply that

$$\int_0^T \|\nabla \Delta \varphi\|_{L^2}^2 dt \leq C \left(1 + \varepsilon^{-4 - \frac{2d}{6-d}} \right).$$

Hence, (3.8) holds. The proof is complete. \square

Remark 3.1. (a) Compare with a priori estimates for the Navier–Stokes–Allen–Cahn phase field model obtained in [18], here for the Navier–Stokes–Cahn–Hilliard model we get better uniform estimates for w , \mathbf{u}_t , and \bar{p} . However, the estimate for φ_t is weaker.

(b) The estimate (3.1) is often known as the mass conservation property of the Cahn–Hilliard equation. It should be noted that this property does not hold for the Navier–Stokes–Allen–Cahn model.

(c) It is well known that no maximum principle holds for the fourth order Cahn–Hilliard equation. Although L^∞ -estimate is known [10] for the Cauchy problem of the Cahn–Hilliard equation, to the best of our knowledge, it is not clear if such an estimate still holds for the initial-boundary value problem for the Cahn–Hilliard equation, in particular, with the presence of a flow. Hence, throughout this paper, we do *not* assume any L^∞ -estimate for φ .

(d). We emphasize that the constant C in (3.2)–(3.8) is independent of T .

The next lemma derives a priori estimates in higher norms for (\mathbf{u}, φ) under stronger assumptions on the initial data $(\mathbf{u}_0^\varepsilon, \varphi_0^\varepsilon)$.

LEMMA 3.2. *In addition to the assumptions of Lemma 3.1, suppose that $\mathbf{u}_0^\varepsilon \in \mathbf{V}$, $\varphi_0^\varepsilon \in H^2(\Omega)$, then every regular solution (\mathbf{u}, φ) of problem (2.1)–(2.3) satisfies the following estimates: for any $T \in (0, \infty)$*

$$(3.15) \quad \operatorname{ess\,sup}_{t \in [0, T]} \|\Delta \varphi(t)\|_{L^2}^2 + \gamma \int_0^T \|\Delta^2 \varphi(s)\|_{L^2}^2 ds \leq c_1 \varepsilon^{-\frac{2d(18-d)}{d^2-24d+72}},$$

$$(3.16) \quad \int_0^T \left[\|\varphi_t(s) + \mathbf{u}(s) \cdot \nabla \varphi(s)\|_{L^2}^2 + \gamma^2 \|\Delta w(s)\|_{L^2}^2 \right] ds \leq c_2 \varepsilon^{-\frac{2d(18-d)}{d^2-24d+72}},$$

$$(3.17) \quad \int_0^T \|\varphi_t(s)\|_{L^2}^2 ds \leq c_3 \varepsilon^{-\frac{2d(18-d)}{d^2-24d+72}}.$$

Moreover, when $d = 2$ there also hold the following additional estimates:

$$(3.18) \quad \operatorname{ess\,sup}_{t \in [0, T]} \|\nabla \mathbf{u}\|_{L^2}^2 + \nu \int_0^T \|\Delta \mathbf{u}(s)\|_{L^2}^2 ds \leq c_4 \varepsilon^{-\frac{2d(18-d)}{d^2-24d+72}},$$

$$(3.19) \quad \int_0^T \left[\|\mathbf{u}_t(s)\|_{L^2}^2 + \|\nabla \bar{p}(s)\|_{L^2}^2 \right] ds \leq c_5 \varepsilon^{-\frac{2d(18-d)}{d^2-24d+72}}.$$

Here $c_j = c_j(u_0, \varphi_0, \nu, g, \lambda, \gamma, T)$ for $j = 1, 2, 3, 4, 5$ are some positive constants.

Proof. Testing (2.2) with $\Delta^2 \varphi$ and using Young's inequality yields

$$(3.20) \quad \frac{d}{dt} \|\Delta \varphi\|_{L^2}^2 + \gamma \|\Delta^2 \varphi\|_{L^2}^2 \leq \frac{\gamma}{\varepsilon^4} \|\Delta f(\varphi)\|_{L^2}^2 + \frac{1}{\gamma} \|\mathbf{u} \cdot \Delta \varphi\|_{L^2}^2.$$

By (3.2) and the interpolation inequality (cf. [1]):

$$\|\nabla \varphi\|_{L^\infty} \leq C \|\Delta^2 \varphi\|_{L^2}^{\frac{d}{6}} \|\nabla \varphi\|_{L^2}^{\frac{6-d}{6}} + C \|\nabla \varphi\|_{L^2},$$

we have

$$(3.21) \quad \begin{aligned} \|\mathbf{u} \cdot \Delta \varphi\|_{L^2}^2 &\leq \|\mathbf{u}\|_{L^2}^2 \|\nabla \varphi\|_{L^\infty}^2 \\ &\leq C \|\Delta^2 \varphi\|_{L^2}^{\frac{d}{3}} \|\nabla \varphi\|_{L^2}^{\frac{6-d}{3}} + C \|\nabla \varphi\|_{L^2}^2 \\ &\leq \frac{\gamma}{4} \|\Delta^2 \varphi\|_{L^2}^2 + C. \end{aligned}$$

To estimate the first term on the right-hand side of (3.20), using the differential identity

$$\Delta f(\varphi) = f'(\varphi)\Delta\varphi + f''(\varphi)|\nabla\varphi|^2,$$

we have

$$\|\Delta f(\varphi)\|_{L^2} \leq 3 \|\varphi\|_{L^\infty}^2 \|\Delta\varphi\|_{L^2} + 6 \|\varphi\|_{L^\infty} \|\nabla\varphi\|_{L^4}^2.$$

The above inequality, (3.2), and the interpolation inequalities (cf. [1])

$$(3.22) \quad \|\varphi\|_{L^\infty} \leq C \left(\|\Delta^2\varphi\|_{L^2}^{\frac{d}{2(12-d)}} \|\varphi\|_{L^6}^{\frac{3(8-d)}{2(12-d)}} + \|\varphi\|_{L^6} \right)$$

$$(3.23) \quad \|\Delta\varphi\|_{L^2} \leq C \left(\|\Delta^2\varphi\|_{L^2}^{\frac{d}{6}} \|\nabla\varphi\|_{L^2}^{\frac{6-d}{6}} + \|\nabla\varphi\|_{L^2} \right)$$

$$(3.24) \quad \|\nabla\varphi\|_{L^4} \leq C \left(\|\Delta^2\varphi\|_{L^2}^{\frac{d}{12}} \|\nabla\varphi\|_{L^2}^{\frac{12-d}{12}} + \|\nabla\varphi\|_{L^2} \right),$$

imply that

$$(3.25) \quad \|\Delta f(\varphi)\|_{L^2} \leq C \left(\|\Delta^2\varphi\|_{L^2}^{\frac{d(18-d)}{6(12-d)}} + 1 \right) \leq \varepsilon^2 \sqrt{\frac{\gamma}{8}} \|\Delta^2\varphi\|_{L^2} + C\varepsilon^{-\frac{2d(18-d)}{d^2-24d+72}}.$$

Now (3.15) follows immediately from combining (3.20), (3.21), and (3.25).

Applying the operator Δ to both sides of (2.9) we get

$$\Delta w = -\Delta^2\varphi + \frac{1}{\varepsilon^2}\Delta f(\varphi).$$

It then follows from the above equation, (3.15), and (3.25) that

$$\int_0^T \|\Delta w(s)\|_{L^2}^2 ds \leq C\varepsilon^{-\frac{2d(18-d)}{d^2-24d+72}},$$

which (2.14) in turn implies that

$$\int_0^T \|\varphi_t(s) + \mathbf{u}(s) \cdot \nabla\varphi(s)\|_{L^2}^2 ds \leq C\varepsilon^{-\frac{2d(18-d)}{d^2-24d+72}}.$$

Hence, (3.16) holds.

Clearly, (3.17) is a trivial consequence of (3.16) and (3.21). To show (3.18), we test (2.13) with $-\Delta\mathbf{u}$ to get

$$(3.26) \quad \frac{1}{2} \frac{d}{dt} \|\nabla\mathbf{u}\|_{L^2}^2 + \nu \|\Delta\mathbf{u}\|_{L^2}^2 = ((\mathbf{u} \cdot \nabla)\mathbf{u}, \Delta\mathbf{u}) + \lambda(\varphi\nabla w, \Delta\mathbf{u}) - (\mathbf{g}, \Delta\mathbf{u}).$$

Using (3.2) and interpolation inequalities, three terms on the right-hand side of (3.26) can be bounded as follows:

$$(3.27) \quad \begin{aligned} |((\mathbf{u} \cdot \nabla)\mathbf{u}, \Delta\mathbf{u})| &\leq \|\Delta\mathbf{u}\|_{L^2} \|\mathbf{u}\|_{L^4} \|\nabla\mathbf{u}\|_{L^4} \\ &\leq C \|\Delta\mathbf{u}\|_{L^2}^{\frac{4+d}{4}} \|\mathbf{u}\|_{L^2}^{\frac{4-d}{4}} \|\nabla\mathbf{u}\|_{L^2}, \quad (\text{see [33]}) \\ &\leq \frac{\nu}{4} \|\Delta\mathbf{u}\|_{L^2}^2 + C \|\nabla\mathbf{u}\|_{L^2}^{2+\frac{2d}{4-d}}, \end{aligned}$$

$$(3.28) \quad \begin{aligned} |\lambda(\varphi\nabla w, \Delta\mathbf{u})| &\leq \|\Delta\mathbf{u}\|_{L^2} \|\nabla w\|_{L^4} \|\phi\|_{L^4} \\ &\leq C \|\Delta\mathbf{u}\|_{L^2} \left\{ \|\Delta w\|_{L^2}^{\frac{d}{4}} \|\nabla w\|_{L^2}^{\frac{4-d}{4}} + \|\nabla w\|_{L^2} \right\} \\ &\leq \frac{\nu}{4} \|\Delta\mathbf{u}\|_{L^2}^2 + C \|\Delta w\|_{L^2}^2 + C \|\nabla w\|_{L^2}^2, \end{aligned}$$

$$(3.29) \quad |(\mathbf{g}, \Delta\mathbf{u})| \leq \frac{\nu}{4} \|\Delta^2\mathbf{u}\|_{L^2}^2 + C \|\mathbf{g}\|_{L^2}^2.$$

For $d = 2$, (3.18) now follows from applying the Gronwall's inequality to (3.26) after substituting (3.27)–(3.29) into it.

Testing (2.13) with \mathbf{u}_t and utilizing (3.2), (3.28), (3.29), and (3.18) we obtain

$$\int_0^T \|\mathbf{u}_t(s)\|_{L^2}^2 ds \leq C \varepsilon^{-\frac{2d(18-d)}{d^2-24d+72}},$$

which together with (2.13), (3.18), and (3.27) in turn implies that

$$\int_0^T \|\nabla \bar{p}(s)\|_{L^2}^2 ds \leq C \varepsilon^{-\frac{2d(18-d)}{d^2-24d+72}}.$$

Hence, (3.19) holds. The proof is complete. \square

Remark 3.2. (a) When $d = 3$, estimates (3.18) and (3.19) only hold local in time as is the case for the Navier–Stokes equations (cf. [33]). In addition, the difficulty of extending these estimates to all times is caused exactly by the nonlinear term $(\mathbf{u} \cdot \nabla)\mathbf{u}$, not by the nonlinear coupling terms.

(b) Unlike the Navier–Stokes–Allen–Cahn model for two-phase fluids (cf. [18]), the higher order norm estimates for the solution of the Navier–Stokes–Cahn–Hilliard model depend on ε^{-1} only *polynomially*, instead of *exponentially*. This important fact may give the possibility to derive a priori error estimates, which depend on ε^{-1} polynomially, for numerical solutions to the Navier–Stokes–Cahn–Hilliard model; see section 4 for further discussions.

4. Fully discrete finite element approximations and convergence analysis. In this section, we shall first give the weak formulation of the problem (2.1)–(2.5) based on the mixed (or split) setting using variables $(\mathbf{u}, \bar{p}, \varphi, w)$. We then introduce a family of fully discrete finite element methods based on this mixed (or split) weak formulation. The implicit Euler time-stepping will be used as a prototype scheme for time discretization and for presenting the idea of our convergence analysis. Essentially, any stable finite element for the Navier–Stokes equations can be used for the spatial discretizations of \mathbf{u} and \bar{p} , and any of Ciarlet–Raviart family of mixed elements for the biharmonic operator can be used for the spatial discretizations of φ and w . The highlight of this section is to establish a discrete energy law, which mimics exactly the basic energy law (3.9) for the Navier–Stokes–Cahn–Hilliard phase field model, for the proposed finite element methods. Utilizing this discrete energy law we then show the convergence of the numerical solutions to the weak solution of (2.13), (2.14), (2.3), and (2.9) as $h, \tau \rightarrow 0$, and to the solution of its sharp interface model (1.1)–(1.4) as $h, \tau, \varepsilon \rightarrow 0$, provided that the phase field model converges to the sharp interface model (cf. Conjecture 4.1).

4.1. Weak formulation. The mixed weak formulation of (2.13), (2.14), (2.3), and (2.9) used in this paper is defined as follows: Find $(\mathbf{u}, \bar{p}, \varphi, w)$ such that

$$\begin{aligned} \mathbf{u} &\in L^\infty((0, T); \mathbf{L}^2(\Omega)) \cap L^2((0, T); \mathbf{H}_0^1(\Omega)) \cap L^2((0, T); \mathbf{V}^*), \\ \int_0^t \bar{p}(s) ds &\in L^\infty((0, T); L_0^2(\Omega)), \\ \varphi &\in L^\infty((0, T); H^1(\Omega)) \cap H^1((0, T); H^{-1}(\Omega)), \\ w &\in L^2((0, T); H^1(\Omega)), \end{aligned}$$

and (2.13) holds in the distribution sense. Moreover, for all $(\mathbf{v}, q, \psi, \chi) \in \mathbf{V} \times L_0^2(\Omega) \times H^1(\Omega) \times H^1(\Omega)$ there hold

$$(4.1) \quad \langle \mathbf{u}_t, \mathbf{v} \rangle + \nu(\nabla \mathbf{u}, \nabla \mathbf{v}) + ((\mathbf{u} \cdot \nabla) \mathbf{u}, \mathbf{v}) + \lambda(\varphi \nabla w, \mathbf{v}) = (\mathbf{g}, \mathbf{v}),$$

$$(4.2) \quad (\operatorname{div} \mathbf{u}, q) = 0,$$

$$(4.3) \quad \langle \varphi_t, \psi \rangle - (\varphi \mathbf{u}, \nabla \psi) + \gamma(\nabla w, \nabla \psi) = 0,$$

$$(4.4) \quad (\nabla \varphi, \nabla \chi) + \frac{1}{\varepsilon^2}(f(\varphi), \chi) = (w, \chi),$$

with the initial conditions $\mathbf{u}(0) = \mathbf{u}_0^\varepsilon$ and $\varphi(0) = \varphi_0^\varepsilon$.

Remark 4.1. (a) We note that the second term on the left-hand side of (4.3) is obtained after performing an integration by parts to the coupling term. It turns out this simple step is quite important for the construction of the finite element methods which not only satisfy the discrete energy law but also fulfill the mass conservation law (see Lemma 4.2).

(b) The well-posedness of (4.1)–(4.4) can be proved by the standard techniques such as the Galerkin method using a priori estimates derived in the previous section (cf. [33]). In fact, as a by-product, our convergence result (see section 4.3) also provides an alternative and constructive proof of the existence of weak solutions.

4.2. Formulation of fully discrete finite element method. Let $J_\tau = \{t_m\}_{m=0}^M$ be a quasi-uniform partition of $[0, T]$ of mesh size $\tau := \frac{T}{M}$, and $d_t v^m := (v^m - v^{m-1})/\tau$. Let \mathcal{T}_h be a quasi-uniform “triangulation” of the domain Ω of mesh size $h \in (0, 1)$ and $\bar{\Omega} = \bigcup_{K \in \mathcal{T}_h} \bar{K}$ ($K \in \mathcal{T}_h$ are tetrahedrons in the case $d = 3$). For a nonnegative integer r , let $P_r(K)$ denote the space of polynomials of degree less than or equal to r on K . We introduce the finite element spaces

$$\begin{aligned} M_h &= \{q_h \in L_0^2(\Omega); q_h|_K \in P_0(K)\}, \\ \mathbf{X}_h &= \{v_h \in \mathbf{C}^0(\bar{\Omega}) \cap \mathbf{H}_0^1(\Omega); \mathbf{v}_h|_K \in \mathbf{P}_2(K)\}, \\ \mathbf{V}_h &= \{\mathbf{v}_h \in \mathbf{X}_h; (\operatorname{div} \mathbf{v}_h, q_h) = 0 \quad \forall q_h \in M_h\}, \\ Y_h &= \{\psi_h \in C^0(\bar{\Omega}); \psi_h|_K \in P_r(K), r \geq 1\}. \end{aligned}$$

It is well known that [9, 25] the P_2 - P_0 mixed finite element space (\mathbf{X}_h, M_h) is a stable pair for the Navier–Stokes equations since it satisfies the inf-sup condition

$$(4.5) \quad \sup_{\mathbf{v}_h \in \mathbf{X}_h} \frac{(\operatorname{div} \mathbf{v}_h, q_h)}{\|\nabla \mathbf{v}_h\|_{L^2}} \geq c \|q_h\|_{L^2} \quad \forall q_h \in M_h.$$

Remark 4.2. The above finite element spaces (\mathbf{X}_h, M_h) are chosen for the convenience of presentation, our convergence analysis in fact holds for *any* stable mixed finite element pairing (\mathbf{X}_h, M_h) for the Navier–Stokes equations. In addition, the convergence analysis also holds for stabilized finite element approximations of the Navier–Stokes equations (cf. [9]).

It is also well known [13, 34, 16, 19] that $Y_h \times Y_h$ is a stable pair for the biharmonic operator and there holds the inf-sup condition

$$(4.6) \quad \sup_{\psi_h \in Y_h} \frac{(\nabla \psi_h, \nabla \chi_h)}{\|\psi_h\|_{H^1}} \geq c \|\chi_h\|_{H^1} \quad \forall \chi_h \in Y_h.$$

We now are ready to introduce our fully discrete mixed finite element methods for problem (2.1)–(2.5). Find $\{(\mathbf{u}_h^m, \bar{p}_h^m, \varphi_h^m, w_h)\}_{m=1}^M \in \mathbf{X}_h \times M_h \times Y_h \times Y_h$ such that

for all $(\mathbf{v}_h, q_h, \psi_h, \chi_h) \in \mathbf{X}_h \times M_h \times Y_h \times Y_h$

$$(4.7) \quad (d_t \mathbf{u}_h^m, \mathbf{v}_h) + \nu(\nabla \mathbf{u}_h^m, \nabla \mathbf{v}_h) + ((\mathbf{u}_h^m \cdot \nabla) \mathbf{u}_h^m, \mathbf{v}_h) + \frac{1}{2} (\mathbf{u}_h^m \operatorname{div} \mathbf{u}_h^m, \mathbf{v}_h) - (\bar{p}_h^m, \operatorname{div} \mathbf{v}_h) + \lambda(\varphi_h^m \nabla w_h^m, \mathbf{v}_h) = (\mathbf{g}(t_m), \mathbf{v}_h),$$

$$(4.8) \quad (\operatorname{div} \mathbf{u}_h^m, q_h) = 0,$$

$$(4.9) \quad (d_t \varphi_h^m, \psi_h) - (\varphi_h^m \mathbf{u}_h^m, \nabla \psi_h) + \gamma(\nabla w_h^m, \nabla \psi_h) = 0,$$

$$(4.10) \quad (\nabla \varphi_h^m, \nabla \chi_h) + \frac{1}{\varepsilon^2} (f_h^m, \chi_h) = (w_h^m, \chi_h),$$

with the initial conditions $\mathbf{u}_h^0 = \mathbf{u}_{0h}$, and $\varphi_h^0 = \varphi_{0h}$. Here

$$(4.11) \quad f_h^m = \frac{1}{4} \{ |\varphi_h^m|^2 + |\varphi_h^{m-1}|^2 - 2 \} \{ \varphi_h^m + \varphi_h^{m-1} \},$$

Remark 4.3. (a) The f_h^m factor in the above scheme can be replaced by $\tilde{f}_h^m := (\varphi_h^m)^3 - \varphi_h^{m-1}$. It is not hard to check that the resulted scheme will still satisfy an almost same discrete energy law that (to be given in the next subsection) satisfied by the above scheme, *provided* that a mesh constraint on τ is met (cf. section 3 of [19]).

(b) The solvability of (4.7)–(4.8) can be verified by using a fixed point argument in finite dimensional spaces (cf. [33]) and the discrete energy law to be given in the next subsection.

4.3. Convergence analysis. Since the phase field model couples two sets of well-known equations, the Navier–Stokes equations and the Cahn–Hilliard equation, it should not be hard to derive a priori error estimates for the above fully discrete mixed finite element schemes using the standard techniques as presented in [6, 25, 26, 33] and in [14, 17, 16]. However, since these standard techniques use the Gronwall type arguments at the end, the anticipated error estimates will definitely depend on $\frac{1}{\varepsilon}$ *exponentially*! Such error estimates clearly are not informative and have no practical usefulness for small ε . We refer interested readers to [19, 20] for more discussions in this direction.

One way to overcome this difficulty is to derive better error estimates which only depend on $\frac{1}{\varepsilon}$ *polynomially*, the best situation one can expect. For the Cahn–Hilliard equation, which is (2.2) with $\mathbf{u} = 0$, such error estimates were obtained in [19, 20] using a nonstandard technique. The key idea of this technique is to make use of a spectrum estimate result for the linearized Cahn–Hilliard operator (cf. [4] and the reference therein). In order to adapt this technique for analyzing the scheme (4.1)–(4.4), one needs a similar spectrum estimate result for the linearized operator associated with the coupled system (2.1)–(2.3). Unfortunately, to our knowledge, such a desired spectrum estimate has not been proved in the literature, although it is believed to be true.

In this paper, we shall take a different approach to address the convergence. Instead of proving the convergence by first establishing a rate of convergence (i.e., an error estimate), we shall prove the convergence directly. As expected, the crux of carrying out such a proof is to derive uniform (in ε) a priori estimates for the numerical solutions; in particular, to establish a discrete energy law, which must mimic the basic energy law (3.9). It should be noted that not every numerical method will meet such a criterion. The goal of this subsection is to prove that the fully discrete finite element method proposed in section 4.2 indeed is one exception. We verify our claim in the

next lemma by establishing a discrete counterpart of the basic energy law (3.9) for the numerical scheme (4.7)–(4.8).

LEMMA 4.1. *Let $(\mathbf{u}_h^m, \bar{p}_h^m, \varphi_h^m, w_h^m)$ solves (4.7)–(4.10), then there holds that*

$$(4.12) \quad \mathcal{J}_{\varepsilon, \lambda}(\mathbf{u}_h^\ell, \varphi_h^\ell) + \tau \sum_{m=1}^{\ell} \left[\frac{\tau}{2} \|d_t \mathbf{u}_h^m\|_{L^2}^2 + \frac{\tau \lambda}{2} \|d_t \nabla \varphi_h^m\|_{L^2}^2 + \nu \|\nabla \mathbf{u}_h^m\|_{L^2}^2 \right. \\ \left. + \lambda \gamma \|\nabla w_h^m\|_{L^2}^2 \right] = \tau \sum_{m=1}^{\ell} (\mathbf{g}(t_m), \mathbf{u}_h^m) + \mathcal{J}_{\varepsilon, \lambda}(\mathbf{u}_h^0, \varphi_h^0)$$

for all $0 \leq \ell \leq M$. Here $\mathcal{J}_{\varepsilon, \lambda}(\cdot, \cdot)$ is defined by (3.10).

Proof. The desired estimate (4.12) follows from setting $\mathbf{v}_h = \mathbf{u}_h^m$ in (4.7), $q_h = \bar{p}_h^m$ in (4.8), $\psi_h = w_h^m$ in (4.9), $\chi_h = d_t \varphi_h^m$ in (4.10), adding the resulting equations, using the identities

$$\begin{aligned} (d_t \mathbf{u}_h^m, \mathbf{u}_h^m) &= \frac{1}{2} \{d_t \|\mathbf{u}_h^m\|_{L^2}^2 + \tau \|d_t \mathbf{u}_h^m\|_{L^2}^2\}, \\ (d_t \nabla \mathbf{u}_h^m, \nabla \mathbf{u}_h^m) &= \frac{1}{2} \{d_t \|\nabla \mathbf{u}_h^m\|_{L^2}^2 + \tau \|d_t \nabla \mathbf{u}_h^m\|_{L^2}^2\}, \\ ((\mathbf{u}_h^m \cdot \nabla) \mathbf{u}_h^m, \mathbf{u}_h^m) + \frac{1}{2} (\mathbf{u}_h^m \operatorname{div} \mathbf{u}_h^m, \mathbf{u}_h^m) &= 0, \\ (d_t \varphi_h^m, f_h^m) &= \frac{1}{4} d_t \|(\varphi_h^m)^2 - 1\|_{L^2}^2. \end{aligned}$$

and applying the operator $\tau \sum_{m=1}^{\ell}$ to the combined equation. \square

The discrete energy law immediately implies the following uniform (in ε) a priori estimates for $(\mathbf{u}_h^m, \bar{p}_h^m, \varphi_h^m, w_h^m)$.

LEMMA 4.2. *Let $(\mathbf{u}_h^m, \bar{p}_h^m, \varphi_h^m, w_h^m)$ solves (4.7)–(4.10), and suppose that $\mathbf{g} \in L^2((0, T); \mathbf{H}^{-1}(\Omega))$ and there exists a positive constant C_0 such that $\mathcal{J}_{\varepsilon, \lambda}(\mathbf{u}_h^0, \varphi_h^0) \leq C_0$, then there hold the following estimates:*

$$(4.13) \quad \int_{\Omega} \varphi_h^m dx = \int_{\Omega} \varphi_h^0, \quad \text{for } m \geq 1,$$

$$(4.14) \quad \max_{0 \leq m \leq M} \{ \|\mathbf{u}_h^m\|_{L^2}^2 + \lambda \|\nabla \varphi_h^m\|_{L^2}^2 + \lambda \varepsilon^{-2} (F(\varphi_h^m), 1) \} \leq C,$$

$$(4.15) \quad \sum_{m=1}^M [\|\mathbf{u}_h^m - \mathbf{u}_h^{m-1}\|_{L^2}^2 + \lambda \|\nabla \varphi_h^m - \nabla \varphi_h^{m-1}\|_{L^2}^2] \leq C,$$

$$(4.16) \quad \tau \sum_{m=1}^M [\nu \|\nabla \mathbf{u}_h^m\|_{L^2}^2 + \lambda \gamma \|\nabla w_h^m\|_{L^2}^2] \leq C,$$

$$(4.17) \quad \tau \sum_{m=1}^M \|d_t \mathbf{u}_h^m\|_{\mathbf{V}^*}^{\frac{12}{6+d}} \leq C,$$

$$(4.18) \quad \max_{0 \leq \ell \leq M} \left\| \tau \sum_{m=1}^{\ell} \bar{p}_h^m \right\|_{L^2} \leq C,$$

$$(4.19) \quad \tau \sum_{m=1}^M \|d_t \varphi_h^m\|_{H^{-1}}^2 \leq C,$$

for some positive constant $C = C(\mathbf{g}, C_0)$.

Proof. Equation (4.13) follows from setting $\psi_h = 1$ in (4.9), and (4.14)–(4.19) are the immediate consequences of the discrete energy law (4.12).

To show (4.17), let P_h denote the L^2 -projection operator from $\mathbf{L}^2(\Omega)$ to \mathbf{V}_h . For any $\mathbf{v} \in \mathbf{V}$ setting $\mathbf{v}_h = P_h \mathbf{v}$ in (4.7), using the stability property of P_h and an inverse inequality (cf. [13, 25]) we get

$$\begin{aligned} (d_t \mathbf{u}_h^m, \mathbf{v}) &= -\nu (\nabla \mathbf{u}_h^m, \nabla P_h \mathbf{v}) - \lambda (\varphi_h^m \nabla w_h^m, P_h \mathbf{v}) - ((\mathbf{u}_h^m \cdot \nabla) \mathbf{u}_h^m, P_h \mathbf{v}) \\ &\quad - \frac{1}{2} (\mathbf{u}_h^m \operatorname{div} \mathbf{u}_h^m, P_h \mathbf{v}) + (\mathbf{g}, P_h \mathbf{v}) \\ &\leq c\nu \|\nabla \mathbf{u}_h^m\|_{L^2} \|\nabla \mathbf{v}\|_{L^2} + \lambda \|\nabla w_h^m\|_{L^2} \|\varphi_h^m\|_{L^3} \|\mathbf{v}\|_{L^6} \\ &\quad + \|\nabla \mathbf{u}_h^m\|_{L^2} \|\mathbf{u}_h^m\|_{L^3} \|\mathbf{v}\|_{L^6} + c \|\mathbf{g}\|_{H^{-1}} \|\nabla \mathbf{v}\|_{L^2} \\ &\leq c\{\nu \|\nabla \mathbf{u}_h^m\|_{L^2} + \lambda \|\nabla w_h^m\|_{L^2} + \|\mathbf{g}\|_{H^{-1}}\} \|\nabla \mathbf{v}\|_{L^2} \\ &\quad + \|\nabla \mathbf{u}_h^m\|_{L^2}^{\frac{6+d}{6}} \|\mathbf{u}_h^m\|_{L^2}^{\frac{6-d}{6}} \|\nabla \mathbf{v}\|_{L^2}. \end{aligned}$$

It follows from the above estimate and (4.14)–(4.16) that

$$\tau \sum_{m=1}^M \|d_t \mathbf{u}_h^m\|_{V^*}^{\frac{12}{6+d}} \leq C.$$

Hence, (4.17) holds.

To show (4.18), we apply the operator $\tau \sum_{m=1}^\ell$ to (4.7) to get

$$\begin{aligned} \left(\tau \sum_{m=1}^\ell \bar{p}_h^m, \operatorname{div} \mathbf{v}_h \right) &= (\mathbf{u}_h^\ell - \mathbf{u}_h^0, \mathbf{v}_h) + \nu \left(\tau \sum_{m=1}^\ell \nabla \mathbf{u}_h^m, \nabla \mathbf{v}_h \right) \\ &\quad + \left(\tau \sum_{m=1}^\ell \left[(\mathbf{u}_h^m \cdot \nabla) \mathbf{u}_h^m + \frac{1}{2} \mathbf{u}_h^m \operatorname{div} \mathbf{u}_h^m \right], \mathbf{v}_h \right) \\ &\quad + \lambda \left(\tau \sum_{m=1}^\ell \varphi_h^m \nabla w_h^m, \mathbf{v}_h \right) - \left(\tau \sum_{m=1}^\ell \mathbf{g}(t_m), \mathbf{v}_h \right). \end{aligned}$$

It then follows from (4.14), (4.16), (3.12), (3.13), and the Sobolev inequality (cf. [1]) that

$$(4.20) \quad \left(\tau \sum_{m=1}^\ell \bar{p}_h^m, \operatorname{div} \mathbf{v}_h \right) \leq C \|\mathbf{v}_h\|_{H^1} \quad \forall \mathbf{v}_h \in \mathbf{X}_h.$$

Hence, (4.18) is an immediate consequence of (4.20) and the inf-sup inequality (4.5).

Finally, to show (4.19), for any $\psi \in H_0^1(\Omega)$ setting $\psi_h = Q_h \psi$ in (4.9), where Q_h denotes the L^2 -projection from $L^2(\Omega)$ to Y_h , and using the stability property of the L^2 -projection (cf. [8]) we get

$$\begin{aligned} (d_t \varphi_h^m, \psi) &= -\gamma (\nabla w_h^m, \nabla Q_h \psi) - (\mathbf{u}_h^m \cdot \nabla \varphi_h^m, \psi) \\ &\leq c\gamma \|\nabla w_h^m\|_{L^2} \|\nabla \psi\|_{L^2} + \|\mathbf{u}_h^m \cdot \nabla \varphi_h^m\|_{L^{\frac{6}{5}}} \|\psi\|_{L^6} \\ &\leq c\{\gamma \|\nabla w_h^m\|_{L^2} + \|\nabla \mathbf{u}_h^m\|_{L^2} \|\nabla \varphi_h^m\|_{L^2}\} \|\nabla \psi\|_{L^2}. \end{aligned}$$

Now, (4.19) follows immediately from the above estimate and (4.14)–(4.16). The proof is complete. \square

Remark 4.4. The property (4.13) says that our numerical methods preserve the mass conservation law of the phase field model (cf. (3.1)). This property will be further validated numerically in section 5. We remark that such a mass conservation law does not hold for the Navier–Stokes–Cahn–Hilliard phase field model, nor does it for its numerical approximations developed in [18].

Let $(\mathbf{U}_{\varepsilon,h,\tau}(x,t), \Phi_{\varepsilon,h,\tau}(x,t))$ denote the piecewise linear interpolation (in t) of the fully discrete solution $\{(\mathbf{u}_h^m, \varphi_h^m)\}$, that is,

$$(4.21) \quad \mathbf{U}_{\varepsilon,h,\tau}(\cdot, t) := \frac{t - t_{m-1}}{\tau} \mathbf{u}_h^m(\cdot) + \frac{t_m - t}{\tau} \mathbf{u}_h^{m-1}(\cdot) \quad \forall t \in [t_{m-1}, t_m],$$

$$(4.22) \quad \Phi_{\varepsilon,h,\tau}(\cdot, t) := \frac{t - t_{m-1}}{\tau} \varphi_h^m(\cdot) + \frac{t_m - t}{\tau} \varphi_h^{m-1}(\cdot) \quad \forall t \in [t_{m-1}, t_m],$$

for $1 \leq m \leq M$, and let $\bar{P}_{\varepsilon,h,\tau}(x,t)$, $\bar{\mathbf{U}}_{\varepsilon,h,\tau}(x,t)$, $\bar{\Phi}_{\varepsilon,h,\tau}(x,t)$, and $\bar{W}_{\varepsilon,h,\tau}(x,t)$ denote the piecewise constant extensions of $\{\bar{p}_h^m\}$, $\{\mathbf{u}_h^m\}$, $\{\varphi_h^m\}$, and $\{w_h^m\}$, respectively. That is,

$$(4.23) \quad \bar{P}_{\varepsilon,h,\tau}(\cdot, t) := \bar{p}_h^m \quad \forall t \in [t_{m-1}, t_m], \quad 1 \leq m \leq M,$$

$$(4.24) \quad \bar{\mathbf{U}}_{\varepsilon,h,\tau}(\cdot, t) := \mathbf{u}_h^m \quad \forall t \in [t_{m-1}, t_m], \quad 1 \leq m \leq M,$$

$$(4.25) \quad \bar{\Phi}_{\varepsilon,h,\tau}(\cdot, t) := \varphi_h^m \quad \forall t \in [t_{m-1}, t_m], \quad 1 \leq m \leq M,$$

$$(4.26) \quad \bar{W}_{\varepsilon,h,\tau}(\cdot, t) := w_h^m \quad \forall t \in [t_{m-1}, t_m], \quad 1 \leq m \leq M.$$

We remark that $\mathbf{U}_{\varepsilon,h,\tau}(x,t)$ and $\Phi_{\varepsilon,h,\tau}(x,t)$ are continuous piecewise polynomial functions in space and time, $\bar{P}_{\varepsilon,h,\tau}(x,t)$, $\bar{\mathbf{U}}_{\varepsilon,h,\tau}(x,t)$, $\bar{\Phi}_{\varepsilon,h,\tau}(x,t)$, and $\bar{W}_{\varepsilon,h,\tau}(x,t)$ are right continuous at the nodes $\{t_m\}$.

The main result of this section is the following convergence theorem.

THEOREM 4.3. *Suppose the assumptions of Lemma 4.2 hold. For each fixed $\varepsilon > 0$, let $(\mathbf{u}_*^\varepsilon, \bar{p}_*^\varepsilon, \varphi_*^\varepsilon, w_*^\varepsilon)$ denote the unique solution of problem (4.1)–(4.4), and $\{(\mathbf{U}_{\varepsilon,h,\tau}, \bar{P}_{\varepsilon,h,\tau}, \bar{\Phi}_{\varepsilon,h,\tau}, \bar{W}_{\varepsilon,h,\tau})\}$ be defined as above. Then we have*

$$(4.27) \quad \lim_{h,\tau \rightarrow 0} \left(\|\mathbf{U}_{\varepsilon,h,\tau} - \mathbf{u}_*^\varepsilon\|_{L^2(L^2)} + \|\Phi_{\varepsilon,h,\tau} - \varphi_*^\varepsilon\|_{L^2(L^2)} + \|\bar{W}_{\varepsilon,h,\tau} - w_*^\varepsilon\|_{L^2(L^2)} \right) = 0,$$

$$(4.28) \quad \int_0^t \bar{P}_{\varepsilon,h,\tau}(s) ds \longrightarrow \int_0^t \bar{p}_*^\varepsilon(s) ds \quad \text{weakly } \star \text{ in } L^\infty((0,T); L^2(\Omega)).$$

Proof. Since the proof is long, we divide it into three steps.

Step 1: Extracting convergent subsequences. The estimates of Lemma 4.2 immediately give the following (uniform in h , τ and ε) estimates:

$$(4.29) \quad \|\bar{\mathbf{U}}_{\varepsilon,h,\tau}\|_{L^\infty(L^2)} + \sqrt{\lambda} \|\nabla \bar{\Phi}_{\varepsilon,h,\tau}\|_{L^\infty(L^2)} + \varepsilon^{-1} \sqrt{\lambda} \|\bar{\Phi}_{\varepsilon,h,\tau}^2 - 1\|_{L^\infty(L^2)} \leq C,$$

$$(4.30) \quad \sqrt{\nu} \|\nabla \bar{\mathbf{U}}_{\varepsilon,h,\tau}\|_{L^2(L^2)} + \sqrt{\lambda \gamma} \|\nabla \bar{W}_{\varepsilon,h,\tau}\|_{L^2(L^2)} \leq C,$$

$$(4.31) \quad \left\| \frac{\partial}{\partial t} \mathbf{U}_{\varepsilon,h,\tau} \right\|_{L^{\frac{12}{5+d}}(V^*)} \leq C,$$

$$(4.32) \quad \left\| \int_0^t \bar{P}_{\varepsilon,h,\tau}(s) ds \right\|_{L^\infty(L^2)} \leq C,$$

$$(4.33) \quad \left\| \frac{\partial}{\partial t} \Phi_{\varepsilon,h,\tau} \right\|_{L^2(H^{-1})} \leq C.$$

Then there exists a convergent subsequence of $\{(\mathbf{U}_{\varepsilon,h,\tau}, \bar{P}_{\varepsilon,h,\tau}, \Phi_{\varepsilon,h,\tau}, \bar{W}_{\varepsilon,h,\tau})\}$ (still denote by the same notation) and a quadruple $(\mathbf{u}^\varepsilon, \bar{p}^\varepsilon, \varphi^\varepsilon, w^\varepsilon)$ such that

$$\begin{aligned}\mathbf{u}^\varepsilon &\in L^\infty((0, T); \mathbf{L}^2(\Omega)) \cap L^2((0, T); \mathbf{H}_0^1(\Omega)) \cap H^1((0, T); \mathbf{V}^*), \\ \varphi^\varepsilon &\in L^\infty((0, T); H^1(\Omega)) \cap H^1((0, T); \mathbf{H}^{-1}(\Omega)), \\ \int_0^t \bar{p}^\varepsilon(s) ds &\in L^\infty((0, T); L_0^2(\Omega)), \\ w^\varepsilon &\in L^2((0, T); H^1(\Omega)),\end{aligned}$$

and

$$(4.34) \quad \begin{aligned}\bar{\mathbf{U}}_{\varepsilon,h,\tau} &\xrightarrow{h,\tau \searrow 0} \mathbf{u}^\varepsilon \quad \text{weakly* in } L^\infty((0, T); \mathbf{L}^2(\Omega)), \\ &\quad \text{strongly in } L^2((0, T); \mathbf{L}^2(\Omega)), \\ &\quad \text{weakly in } L^2((0, T); \mathbf{H}^1(\Omega)), \\ &\quad \text{weakly in } H^1((0, T); \mathbf{V}^*),\end{aligned}$$

$$(4.35) \quad \begin{aligned}\bar{\Phi}_{\varepsilon,h,\tau} &\xrightarrow{h,\tau \searrow 0} \varphi^\varepsilon \quad \text{weakly* in } L^\infty((0, T); H^1(\Omega)), \\ &\quad \text{strongly in } L^2((0, T); L^2(\Omega)), \\ &\quad \text{weakly in } H^1((0, T); H^{-1}(\Omega)),\end{aligned}$$

$$(4.36) \quad \int_0^t \bar{P}_{\varepsilon,h,\tau}(s) ds \xrightarrow{h,\tau \searrow 0} \int_0^t \bar{p}^\varepsilon(s) ds \quad \text{weakly * in } L^\infty((0, T); L^2(\Omega)),$$

$$(4.37) \quad \begin{aligned}\bar{W}_{\varepsilon,h,\tau} &\xrightarrow{h,\tau \searrow 0} w^\varepsilon \quad \text{weakly in } L^2((0, T); H^1(\Omega)), \\ &\quad \text{strongly in } L^2((0, T); L^2(\Omega)).\end{aligned}$$

From (4.15) we also have

$$\begin{aligned}\|\mathbf{U}_{\varepsilon,h,\tau} - \bar{\mathbf{U}}_{\varepsilon,h,\tau}\|_{L^2(L^2)}^2 &= \sum_{m=1}^M \|\mathbf{u}_h^m - \mathbf{u}_h^{m-1}\|_{L^2}^2 \int_{t_{m-1}}^{t_m} \left(\frac{t - t_{m-1}}{\tau} \right)^2 dt \\ &= \frac{\tau}{3} \sum_{m=1}^M \|\mathbf{u}_h^m - \mathbf{u}_h^{m-1}\|_{L^2}^2 \xrightarrow{\tau \searrow 0} 0, \\ \|\nabla(\Phi_{\varepsilon,h,\tau} - \bar{\Phi}_{\varepsilon,h,\tau})\|_{L^2(L^2)}^2 &= \frac{\tau}{3} \sum_{m=1}^M \|\nabla(\varphi_h^m - \varphi_h^{m-1})\|_{L^2}^2 \xrightarrow{\tau \searrow 0} 0.\end{aligned}$$

Hence, the sequences $\{\mathbf{U}_{\varepsilon,h,\tau}\}$ and $\{\bar{\mathbf{U}}_{\varepsilon,h,\tau}\}$ converge to the same limit as $h, \tau \rightarrow 0$, so do the sequences $\{\Phi_{\varepsilon,h,\tau}\}$ and $\{\bar{\Phi}_{\varepsilon,h,\tau}\}$.

Step 2: Passing to the limit. We now want to pass to the limit in (4.7)–(4.10) and show that $(\mathbf{u}^\varepsilon, \bar{p}^\varepsilon, \varphi^\varepsilon, w^\varepsilon)$ is a weak solution of problem (4.1)–(4.4) with the initial values $\mathbf{u}^\varepsilon(0) = \mathbf{u}_0^\varepsilon$ and $\varphi^\varepsilon(0) = \varphi_0^\varepsilon$. To the end, we rewrite (4.7)–(4.10) as

$$(4.38) \quad \begin{aligned}((\mathbf{U}_{\varepsilon,h,\tau})_t, \mathbf{v}_h) + \nu(\nabla \bar{\mathbf{U}}_{\varepsilon,h,\tau}, \nabla \mathbf{v}_h) + ((\bar{\mathbf{U}}_{\varepsilon,h,\tau} \cdot \nabla) \bar{\mathbf{U}}_{\varepsilon,h,\tau}, \mathbf{v}_h) \\ + \frac{1}{2} (\bar{\mathbf{U}}_{\varepsilon,h,\tau} \operatorname{div} \bar{\mathbf{U}}_{\varepsilon,h,\tau}, \mathbf{v}_h) + \lambda(\bar{\Phi}_{\varepsilon,h,\tau} \nabla \bar{W}_{\varepsilon,h,\tau}, \mathbf{v}_h) = (\bar{\mathbf{g}}_\tau, \mathbf{v}_h),\end{aligned}$$

$$(4.39) \quad (\operatorname{div} \bar{\mathbf{U}}_{\varepsilon,h,\tau}, q_h) = 0,$$

$$(4.40) \quad ((\Phi_{\varepsilon,h,\tau})_t, \psi_h) - (\bar{\Phi}_{\varepsilon,h,\tau} \bar{\mathbf{U}}_{\varepsilon,h,\tau}, \nabla \psi_h) + \gamma(\nabla \bar{W}_{\varepsilon,h,\tau}, \nabla \psi_h) = 0,$$

$$(4.41) \quad (\nabla \bar{\Phi}_{\varepsilon,h,\tau}, \nabla \chi_h) + \frac{1}{\varepsilon^2} (\bar{f}_{\varepsilon,h,\tau}, \chi_h) = (\bar{W}_{\varepsilon,h,\tau}, \chi_h),$$

for $(\mathbf{v}_h, q_h, \psi_h, \chi_h) \in \mathbf{V}_h \times M_h \times Y_h \times Y_h$. Here $\bar{f}_{\varepsilon, h, \tau}$ and \bar{g}_τ denotes the constant extensions of $\{f_h^m\}$ and $\{\mathbf{g}(t_m)\}$, respectively.

For any $\eta \in C^0[0, T]$, we multiply (4.38)–(4.41) by η , respectively, and integrate the resulting equations in t from 0 to T to get

$$(4.42) \quad \int_0^T [((\mathbf{U}_{\varepsilon, h, \tau})_t, \mathbf{v}_h) + \nu(\nabla \bar{\mathbf{U}}_{\varepsilon, h, \tau}, \nabla \mathbf{v}_h) + ((\bar{\mathbf{U}}_{\varepsilon, h, \tau} \cdot \nabla) \bar{\mathbf{U}}_{\varepsilon, h, \tau}, \mathbf{v}_h)] \eta(t) dt \\ + \int_0^T \left[\frac{1}{2} (\bar{\mathbf{U}}_{\varepsilon, h, \tau} \operatorname{div} \bar{\mathbf{U}}_{\varepsilon, h, \tau}, \mathbf{v}_h) + \lambda (\bar{\Phi}_{\varepsilon, h, \tau} \nabla \bar{W}_{\varepsilon, h, \tau}, \mathbf{v}_h) \right] \eta(t) dt \\ = \int_0^T (\bar{\mathbf{g}}_\tau, \mathbf{v}_h) \eta(t) dt,$$

$$(4.43) \quad \int_0^T (\operatorname{div} \bar{\mathbf{U}}_{\varepsilon, h, \tau}, q_h) \eta(t) dt = 0,$$

$$(4.44) \quad \int_0^T [((\Phi_{\varepsilon, h, \tau})_t, \psi_h) - (\bar{\Phi}_{\varepsilon, h, \tau} \bar{\mathbf{U}}_{\varepsilon, h, \tau}, \nabla \psi_h) + \gamma (\nabla \bar{W}_{\varepsilon, h, \tau}, \nabla \psi_h)] \eta(t) dt = 0,$$

$$(4.45) \quad \int_0^T \left[(\nabla \bar{\Phi}_{\varepsilon, h, \tau}, \nabla \chi_h) + \frac{1}{\varepsilon^2} (\bar{f}_{\varepsilon, h, \tau}, \chi_h) \right] \eta(t) dt = \int_0^T (\bar{W}_{\varepsilon, h, \tau}, \chi_h) \eta(t) dt.$$

For any $(\mathbf{v}, q, \psi, \chi) \in \mathbf{V} \times L_0^2(\Omega) \times H^1(\Omega) \times H^1(\Omega)$, let $(\mathbf{v}_h, q_h, \psi_h, \chi_h) \in \mathbf{V}_h \times M_h \times Y_h \times Y_h$ denote the standard finite element (nodal) interpolations of $(\mathbf{v}, q, \psi, \chi)$ in (4.42)–(4.45). Since

$$\begin{aligned} \mathbf{v}_h &\xrightarrow{h \searrow 0} \mathbf{v} \quad \text{strongly in } \mathbf{H}_0^1(\Omega), \\ q_h &\xrightarrow{h \searrow 0} q \quad \text{strongly in } L_0^2(\Omega), \\ \psi_h &\xrightarrow{h \searrow 0} \psi \quad \text{strongly in } H^1(\Omega), \\ \chi_h &\xrightarrow{h \searrow 0} \chi \quad \text{strongly in } H^1(\Omega), \end{aligned}$$

setting $h, \tau \rightarrow 0$ in (4.42)–(4.45) and using (4.34)–(4.37) we get $\mathbf{u}^\varepsilon(0) = \mathbf{u}_0^\varepsilon$, $\varphi^\varepsilon(0) = \varphi_0^\varepsilon$, and

$$\begin{aligned} &\int_0^T \left[\langle \mathbf{u}_t^\varepsilon, \mathbf{v} \rangle + \nu(\nabla \mathbf{u}^\varepsilon, \nabla \mathbf{v}) + ((\mathbf{u}^\varepsilon \cdot \nabla) \mathbf{u}, \mathbf{v}) + \frac{1}{2} (\mathbf{u}^\varepsilon \operatorname{div} \mathbf{u}^\varepsilon, \mathbf{v}) \right] \eta(t) dt \\ &\quad + \lambda \int_0^T (\varphi^\varepsilon \nabla w^\varepsilon, \mathbf{v}) \eta(t) dt = \int_0^T (\mathbf{g}, \mathbf{v}) \eta(t) dt, \\ &\int_0^T (\operatorname{div} \mathbf{u}^\varepsilon, q) \eta(t) dt = 0, \\ &\int_0^T [\langle \varphi_t, \psi \rangle - (\varphi^\varepsilon \mathbf{u}^\varepsilon, \nabla \psi) + \gamma (\nabla w^\varepsilon, \nabla \psi)] \eta(t) dt = 0, \\ &\int_0^T \left[(\nabla \varphi^\varepsilon, \nabla \chi) + \frac{1}{\varepsilon^2} (f(\varphi^\varepsilon), \chi) \right] \eta(t) dt = \int_0^T (w^\varepsilon, \chi) \eta(t) dt, \end{aligned}$$

which is equivalent to (4.1)–(4.4) since $C^0[0, T]$ is dense in $L^2(0, T)$. In addition, it is easy to see that $(\mathbf{u}^\varepsilon, \bar{p}^\varepsilon, \varphi^\varepsilon, w^\varepsilon)$ satisfies (2.13) in the distribution sense. Hence, $(\mathbf{u}^\varepsilon, \bar{p}^\varepsilon, \varphi^\varepsilon, w^\varepsilon)$ is a weak solution of (4.1)–(4.4).

Step 3: Finishing up. We have shown above that $\{(\mathbf{U}_{\varepsilon,h,\tau}, \bar{P}_{\varepsilon,h,\tau}, \Phi_{\varepsilon,h,\tau}, \bar{W}_{\varepsilon,h,\tau})\}$ has a convergent subsequence and its limit $(\mathbf{u}^\varepsilon, \bar{p}^\varepsilon, \varphi^\varepsilon, w^\varepsilon)$ is a weak solution of (4.1)–(4.4). By the uniqueness, we have $\mathbf{u}^\varepsilon = \mathbf{u}_*^\varepsilon, \bar{p}^\varepsilon = \bar{p}_*^\varepsilon, \varphi^\varepsilon = \varphi_*^\varepsilon$, and $w^\varepsilon = w_*^\varepsilon$. Moreover, the proof also implies that the limit of *every* convergent subsequence of $\{(\mathbf{U}_{\varepsilon,h,\tau}, \bar{P}_{\varepsilon,h,\tau}, \Phi_{\varepsilon,h,\tau}, \bar{W}_{\varepsilon,h,\tau})\}$ must be a weak solution of (4.1)–(4.4). Hence, the whole sequence $\{(\mathbf{U}_{\varepsilon,h,\tau}, \bar{P}_{\varepsilon,h,\tau}, \Phi_{\varepsilon,h,\tau}, \bar{W}_{\varepsilon,h,\tau})\}$ converge to the unique weak solution $(\mathbf{u}_*^\varepsilon, \bar{p}_*^\varepsilon, \varphi_*^\varepsilon, w_*^\varepsilon)$. The proof is complete. \square

Remark 4.5. We remark that since the phase field model (2.13), (2.14), (2.3), and (2.9) contains the Navier–Stokes equations, in general, one cannot expect any better results than those for the Navier–Stokes equations. Hence, the uniqueness assumption on the solution $(\mathbf{u}_*^\varepsilon, \bar{p}_*^\varepsilon, \varphi_*^\varepsilon, w_*^\varepsilon)$ can only be justified when $d = 2$. For the case $d = 3$, it can be shown that (2.13), (2.14), (2.3), and (2.9) has a unique local-in-time classical solution, hence, we assume that the uniqueness is understood local-in-time when $d = 3$. Clearly, without the uniqueness assumption *Step 3* of the above proof does not stand anymore, hence, the convergence stated in Theorem 4.3 only holds for a subsequence, instead of the whole sequence, of $\{(\mathbf{U}_{\varepsilon,h,\tau}, \bar{P}_{\varepsilon,h,\tau}, \Phi_{\varepsilon,h,\tau}, \bar{W}_{\varepsilon,h,\tau})\}$.

We now recall that the following convergent result was conjectured in [27, 30], and we also believe it should be true.

CONJECTURE 4.1. *Assume that the sharp interface problem (1.1)–(1.4) has a unique regular solution (u_*, p_*) . Under the assumptions of Theorem 4.3 there hold*

$$(4.46) \quad \lim_{\varepsilon \rightarrow 0} \|\mathbf{u}_*^\varepsilon - u_*\|_{L^2(L^2)} = 0,$$

$$(4.47) \quad \int_0^t \bar{p}_*^\varepsilon(s) ds \xrightarrow{\varepsilon \searrow 0} \int_0^t p_*(s) ds \quad \text{weakly * in } L^\infty((0, T); L^2(\Omega)),$$

$$(4.48) \quad \varphi_*^\varepsilon \xrightarrow{\varepsilon \searrow 0} \pm 1 \quad \text{a.e. in } \Omega_t^\pm \times (0, T).$$

Here Ω_t^+ and Ω_t^- denote the outside and inside of Γ_t in Ω at time t , respectively.

An immediate consequence of Theorem 4.3 and Conjecture 4.1 is the following convergence theorem.

THEOREM 4.4. *Under the assumptions of Conjecture 4.1 there hold*

$$(4.49) \quad \lim_{\varepsilon \rightarrow 0} \lim_{h, \tau \rightarrow 0} \|\mathbf{U}_{\varepsilon,h,\tau} - u_*\|_{L^2(L^2)} = 0,$$

$$(4.50) \quad \int_0^t \bar{P}_{\varepsilon,h,\tau}(s) ds \xrightarrow{\varepsilon \searrow 0} \int_0^t p_*(s) ds \quad \text{weakly * in } L^\infty((0, T); L^2(\Omega)),$$

$$(4.51) \quad \Phi_{\varepsilon,h,\tau} \xrightarrow{\varepsilon, h, \tau \searrow 0} \pm 1 \quad \text{a.e. in } \Omega_t^\pm \times (0, T).$$

Remark 4.6. (a) The convergence result of Theorem 4.3 essentially guarantees that the numerical solution $(\mathbf{U}_{\varepsilon,h,\tau}, \bar{P}_{\varepsilon,h,\tau}, \Phi_{\varepsilon,h,\tau}, \bar{W}_{\varepsilon,h,\tau})$ enjoys the same kind convergence to the solution (\mathbf{u}_*, p_*) of the sharp interface problem (1.1)–(1.4) as the phase field solution $(\mathbf{u}_*^\varepsilon, \bar{p}_*^\varepsilon, \varphi_*^\varepsilon, w_*^\varepsilon)$ of (2.13), (2.14), (2.3), and (2.9) does.

(b) We remark that the analogue of convergence result (4.50) for the pressure does not hold for the Navier–Stokes–Allen–Cahn model (cf. [18]). However, this result holds for the Navier–Stokes–Cahn–Hilliard model due to the uniform (in ε) estimate (4.18).

5. Numerical experiments. In this section we provide some 2-D numerical experiments to gauge the fully discrete finite element method developed in the previous sections. In addition, our numerical results reveal some interesting features such

as shrinking, splitting, and merging of fluid interfaces governed by the phase field model (2.13), (2.14), (2.3), and (2.9). In all numerical experiments to be given in the following, we choose $\Omega = [-0.4, 0.4]^2$, $\varepsilon = 10^{-2}$, $\nu = 1$, $\lambda = \gamma = 0.1$, $\mathbf{g} = (1, 0)^t$, $u_0^\varepsilon \equiv 0$, while the initial condition for ϕ is specified in each test. Also, in order to resolve the diffuse interface, we use $\tau = 10^{-5}$ and unstructured spatial meshes with the minimum triangle size $h = 10^{-4}$ in all experiments.

Test 1. In this test, we take the following initial condition for φ :

$$\varphi_0^\varepsilon(x) = \tanh\left(\frac{x_1^2}{0.01} + \frac{x_2^2}{0.0225} - 1\right).$$

Note that the zero level set of φ_0^ε , which gives the initial fluid interface, is the ellipse $\frac{x_1^2}{0.01} + \frac{x_2^2}{0.0225} = 1$. Hence, we have the situation of one elliptical fluid bubble inside another fluid.

Figure 5.1 shows snapshots of color and zero-level set plots of the computed phase function ϕ_h^m at six time steps. In the figure, the red color stands for $\phi_h^m = 1$, the blue color stands for $\phi_h^m = -1$, and the black curve represents the zero-level set of the computed phase function. We notice that the elliptical bubble quickly deforms into a circular bubble while the total mass (the integral of ϕ_h^m over Ω) remains constant in time. In the test, we have

$$\int_{\Omega} \phi_h^m dx \equiv 0.54538 \quad \text{for } m = 1, 2, \dots, M.$$

The shape and size of the circular bubble remains unchanged, it should eventually be stabilized (i.e., converge to a stationary solution) due to the dissipative mechanism of the phase field model (2.13), (2.14), (2.3), and (2.9) (cf. Lemma 3.1). We also remark that the interface (zero-level set of φ_h^m) movement is very similar to that of the zero-level set of the solution to the Cahn–Hilliard equation (the equation obtained by setting $u \equiv 0$ in (2.2)) (cf. [21, 22]). As expected, here the zero-level set is pushed to the right by the fluid flow (through the convective term $u \cdot \nabla \phi$) while it is approaching the equilibrium state.

Figure 5.2 displays snapshots of the arrow and streamline plots of the computed velocity field u_h^m at six time steps. The black ellipse in the center of each snapshot stands for the initial fluid interface (i.e., the zero-level set of ϕ_0^ε). We notice that fluid vertices are formed shortly after the initial time step, and the vertices become stronger as the time goes on.

Test 2. In this test, the initial profile of the phase function is taken as

$$\varphi_0^\varepsilon(x) = \tanh\left(\frac{1}{\varepsilon} \left(\frac{x_1^2}{0.0064} + \frac{x_2^2}{0.0225} - 1\right) \left(\frac{x_1^2}{0.0225} + \frac{x_2^2}{0.0064} - 1\right)\right).$$

Note that the zero level set of φ_0^ε , which gives the initial fluid interface, is the union of the following two intersecting ellipses: $\frac{x_1^2}{0.0064} + \frac{x_2^2}{0.0225} = 1$ and $\frac{x_1^2}{0.0225} + \frac{x_2^2}{0.0064} = 1$, which enclose four bullethead-like bubbles inside a fluid.

Figure 5.3 shows snapshots of color and zero-level set plots of the computed phase function φ_h^m at fifteen time steps. Again, the red color stands for $\varphi_h^m = 1$, the blue color stands for $\varphi_h^m = -1$, and the black curve represents the zero-level set of the computed phase function. In this test, we see the fluid bubble first splits into four bubbles, they then deform into four circular bubbles, and finally merge to form a

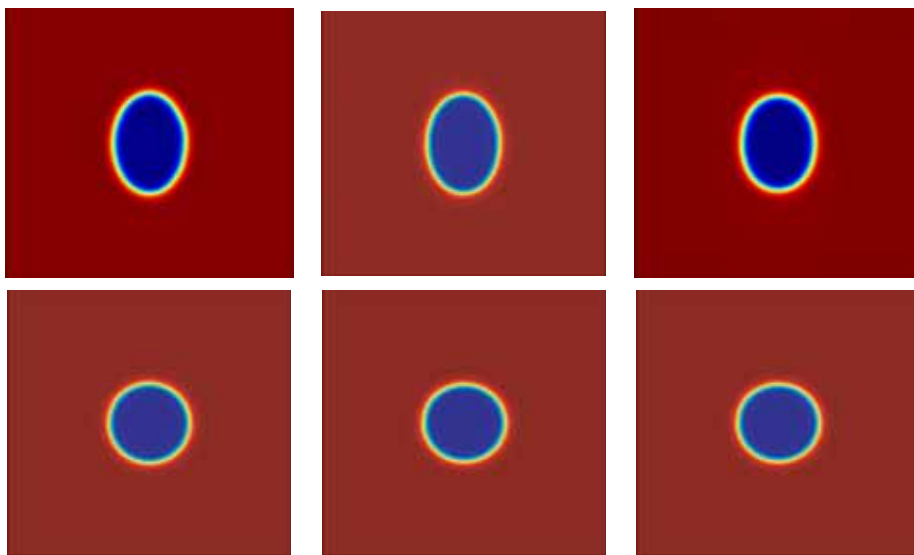


FIG. 5.1. Color and zero-level set plots of computed phase function ϕ_h^m at $t_m = 10^{-7}, 1.1 \times 10^{-6}, 10^{-5}, 10^{-4}, 5 \times 10^{-4}, 10^{-3}$. The graphs are arranged row-wise.

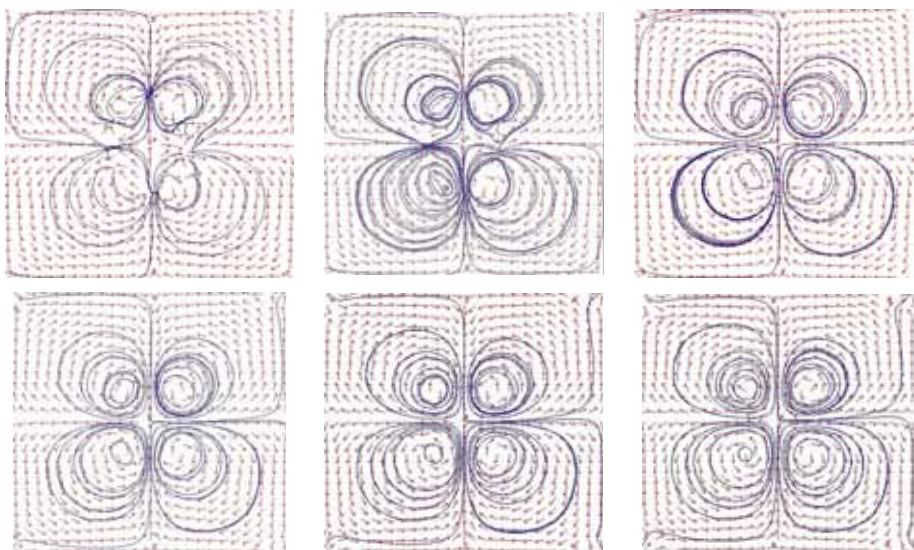


FIG. 5.2. Arrow and streamline plots of computed velocity field u_h^m at $t_m = 10^{-7}, 1.1 \times 10^{-6}, 5 \times 10^{-5}, 2 \times 10^{-4}, 5 \times 10^{-4}, 10^{-3}$. The graphs are arranged row-wise.

bigger circular bubble which eventually stabilizes. During the evolution, the total mass (the integral of ϕ_h^m over Ω) remains constant in time. In the test, we have

$$\int_{\Omega} \phi_h^m dx \equiv 0.58313 \quad \text{for } m = 1, 2, \dots, M.$$

As expected, the interface (zero-level set of ϕ_h^m) movement is very similar to that of the zero-level set of the solution to the Cahn–Hilliard equation (the equation obtained

by setting $u \equiv 0$ in (2.2)) (cf. [21, 22]), and it is pushed very slowly off the center to the right by the fluid flow (through the convective term $u \cdot \nabla \varphi$). Another noticeable difference is that, unlike the dynamics of the zero-level set of the solution to the Cahn–Hilliard equation, here the four bullethead-like bubbles seem to evolve at slightly different speed and the bottom bubble disappears a couple of time steps earlier than the top one, which in turn is taken a couple of time steps earlier than the left bubble. We think that this phenomenon is caused by the fluid flow through the convective term $u \cdot \nabla \varphi$.

Figure 5.4 displays snapshots of the arrow and streamline plots of the computed velocity field u_h^m at nine time steps. The black ellipses in the center of each snapshot stand for the initial fluid interface (i.e., the zero-level set of φ_0^ε). We notice that fluid vertices are formed shortly after the initial time step, and more vertices are produced as the time goes on.

Acknowledgment. The author would like to thank the referees for their helpful comments and suggestions.

REFERENCES

- [1] R. A. ADAMS, *Sobolev Spaces*, Academic press, New York, 1975.
- [2] D. M. ANDERSON AND G. B. MCFADDEN, *A diffuse-interface description of internal waves in a near-critical fluid*, Phys. Fluids, 9 (1997), pp. 1870–1879.
- [3] D. M. ANDERSON, G. B. MCFADDEN, AND A. A. WHEELER, *Diffuse-interface methods in fluid mechanics*, Ann. Rev. Fluid Mech., 30 (1998), pp. 139–165.
- [4] N. D. ALIKAKOS, P. W. BATES, AND X. CHEN, *Convergence of the Cahn–Hilliard equation to the Hele–Shaw model*, Arch. Rational Mech. Anal., 128 (1994), pp. 165–205.
- [5] J. W. BARRETT, X. FENG, AND A. PROHL, *Convergence of a fully discrete finite element approximation of an Ericksen–Leslie model for the flow of liquid crystals*, Numer. Math., submitted.
- [6] J. BERCOVIER AND O. PIRONNEAU, *Error estimates for finite element solution of the Stokes problem in the primitive variables*, Numer. Math., 33 (1979), pp. 211–224.
- [7] J. BEAR, *Dynamics of Fluids in Porous Media*, Dover Publications, Inc., New York, 1972.
- [8] J. H. BRAMBLE AND J. XU, *Some estimates for a weighted L^2 projection*, Math. Comp., 56 (1991), pp. 463–576.
- [9] F. BREZZI AND M. FORTIN, *Mixed and Hybrid Finite Element Methods*, Springer-Verlag, New York, 1991.
- [10] L. A. CAFFARELLI AND N. E. MULER, *An L^∞ bound for solutions of the Cahn–Hilliard equation*, Arch. Rational Mech. Anal., 133 (1995), pp. 129–144.
- [11] J. W. CAHN AND J. E. HILLIARD, *Free energy of a nonuniform system. I. Interfacial free energy*, J. Chem. Phys., 28 (1958), pp. 258–267.
- [12] G. CAGINALP, *An analysis of a phase field model of a free boundary*, Arch. Rational Mech. Anal., 92 (1986), pp. 205–245.
- [13] P. G. CIARLET, *The Finite Element Method for Elliptic Problems*, North-Holland, Amsterdam, 1978.
- [14] Q. DU AND R. A. NICOLAIDES, *Numerical analysis of a continuum model of phase transition*, SIAM J. Numer. Anal., 28 (1991), pp. 1310–1322.
- [15] D. A. EDWARDS, H. BRENNER, AND D. T. WASAN, *Interfacial Transport Process and Rheology*, Butterworths/Heinemann, London, 1991.
- [16] C. M. ELLIOTT, D. A. FRENCH, AND F. A. MILNER, *A second order splitting method for the Cahn–Hilliard equation*, Numer. Math., 54 (1989), pp. 575–590.
- [17] C. M. ELLIOTT AND Z. SONGMU, *On the Cahn–Hilliard equation*, Arch. Rational Mech. Anal., 96 (1986), pp. 339–357.
- [18] X. FENG, Y. HE, AND C. LIU, *Analysis of finite element approximations of a phase field model for two-phase fluids*, Math. Comp., accepted.
- [19] X. FENG AND A. PROHL, *Error analysis of a mixed finite element method for the Cahn–Hilliard equation*, Numer. Math., 99 (2004), pp. 47–84.
- [20] X. FENG AND A. PROHL, *Numerical analysis of the Cahn–Hilliard equation and approximation of the Hele–Shaw problem*, Interfaces Free Bound., 7 (2005), pp. 1–28.

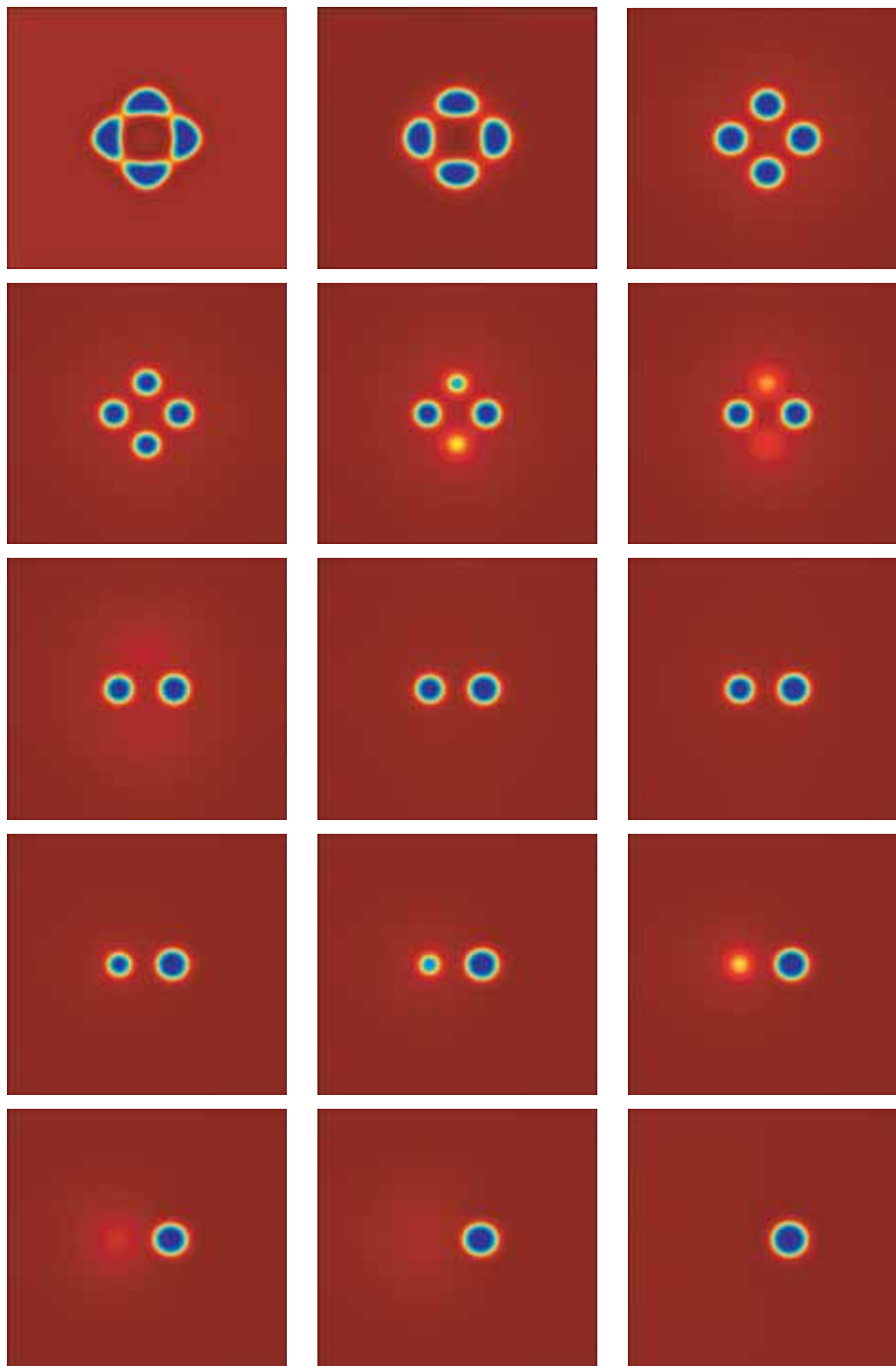


FIG. 5.3. Color and zero-level set plots of computed phase function φ_h^m at $t_m = 10^{-7}, 10^{-6}, 10^{-5}, 3 \times 10^{-5}, 4.2 \times 10^{-5}, 4.3 \times 10^{-5}, 4.5 \times 10^{-5}, 5.5 \times 10^{-5}, 5.8 \times 10^{-5}, 7 \times 10^{-5}, 7.5 \times 10^{-5}, 7.6 \times 10^{-5}, 7.8 \times 10^{-5}, 8 \times 10^{-5}, 9 \times 10^{-5}$. The graphs are arranged row-wise.

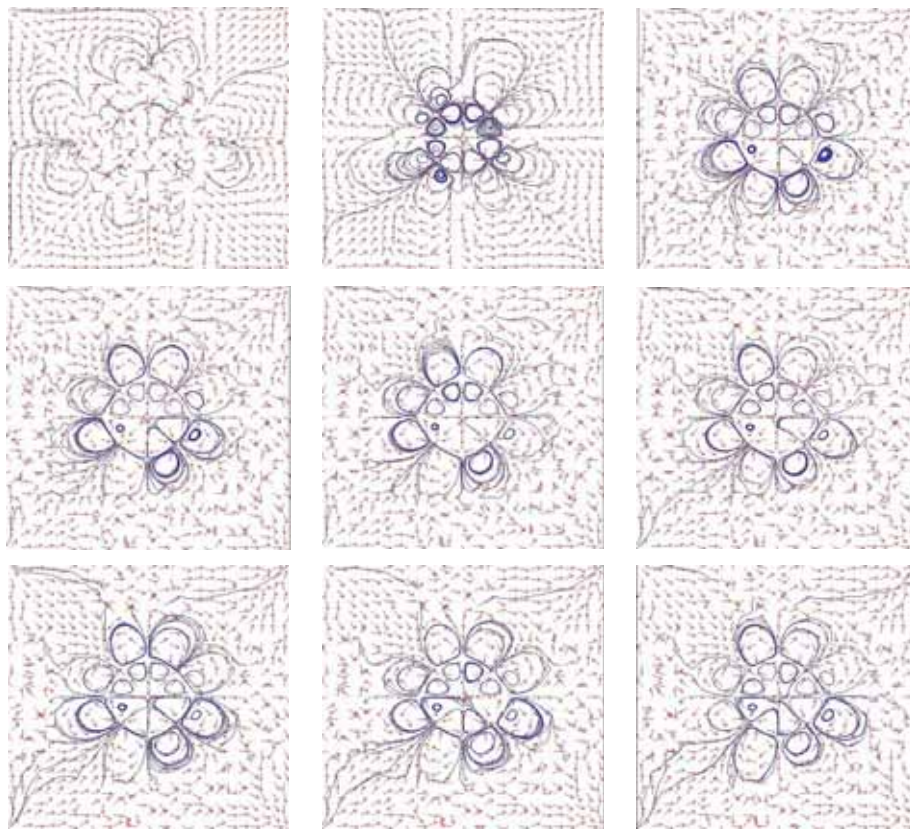


FIG. 5.4. Arrow and streamline plots of computed velocity field u_h^n at $t_m = 10^{-7}, 10^{-6}, 10^{-5}, 3 \times 10^{-5}, 4 \times 10^{-5}, 5 \times 10^{-5}, 7 \times 10^{-5}, 8 \times 10^{-5}, 9 \times 10^{-5}$. The graphs are arranged row-wise.

- [21] X. FENG AND A. PROHL, *Analysis of a fully discrete finite element method for the phase field model and approximation of its sharp interface limits*, Math. Comp., 73 (2003), pp. 541–567.
- [22] X. FENG AND H. WU, *A posteriori error estimates for finite element approximations of the Cahn–Hilliard equation and the Hele–Shaw flow*, M²AN, submitted.
- [23] P. FIFE, *Dynamics of Internal Layers and Diffusive Interfaces*, SIAM, Philadelphia, 1988.
- [24] G. FIX, *Phase field method for free boundary problems*, in Free Boundary Problems, A. Fasano and M. Primicerio, eds., Pitman, London, 1983, pp. 580–589.
- [25] V. GIRAULT AND P. A. RAVIART, *Finite Element Method for Navier–Stokes Equations: Theory and algorithms*, Springer-Verlag, Berlin, Heidelberg, New York, 1981.
- [26] J. G. HEYWOOD AND R. RANNACHER, *Finite element approximation of the nonstationary Navier–Stokes problem. I. Regularity of solutions and second-order error estimates for spatial discretization*, SIAM J. Numer. Anal., 19 (1982), pp. 275–311.
- [27] D. JACQMIN, *Calculation of two-phase Navier–Stokes flows using phase-field modeling*, J. Comput. Phys., 155 (1999), pp. 96–127.
- [28] J. S. LANGER, *Models of patten formation in first-order phase transitions*, in Directions in Condensed Matter Physics, World Science Publishers, 1986, pp. 164–186.
- [29] G. M. LIEBERMAN, *Second Order Parabolic Differential Equations*, World Scientific Publishing, Singapore, 1996.
- [30] C. LIU AND J. SHEN, *A phase field model for the mixture of two incompressible fluids and its approximation by a Fourier-spectral method*, Phys. D, 179 (2003), pp. 211–228.
- [31] J. LOWENGRUB AND I. TRUSKINOVSKY, *Quasi-incompressible Cahn–Hilliard fluids and topological transitions*, R. Soc. Lond. Proc. Ser. A Math. Phys. Eng. Sci., 454 (1998), pp. 2617–2654.
- [32] G. B. MCFADDEN, *Phase-field models of solidification*, Contemp. Math., 306, 295 (2002), pp. 107–145.

- [33] R. TEMAM, *Navier–Stokes Equations*, Theory and Numerical Analysis, AMS Chelsea Publishing, Providence, RI, 2001.
- [34] R. SCHOLZ, *A mixed method for 4th order problems using linear finite elements*, RAIRO Anal. Numér., 12 (1978), pp. 85–90.